US009622913B2

(12) **United States Patent**
Chaudhary et al.

(10) **Patent No.: US 9,622,913 B2**
(45) **Date of Patent: Apr. 18, 2017**

(54) **IMAGING-CONTROLLED LASER SURGICAL SYSTEM**

(75) Inventors: **Gautam Chaudhary**, Laguna Hills, CA (US); **Peter Goldstein**, Santa Ana, CA (US); **Imre Hegedus**, Budapest (HU); **Carlos German Suárez**, Tustin, CA (US); **David Calligori**, Rancho Santa Margarita, CA (US); **Michael Karavitis**, Dana Point, CA (US)

(73) Assignee: **Alcon LenSx, Inc.**, Aliso Viejo, CA (US)

(*) Notice: Subject to any disclaimer, the term of this patent is extended or adjusted under 35 U.S.C. 154(b) by 159 days.

(21) Appl. No.: **13/110,352**

(22) Filed: **May 18, 2011**

(65) **Prior Publication Data**

US 2012/0296319 A1 Nov. 22, 2012

(51) **Int. Cl.**

A61F 9/008	(2006.01)
A61B 3/14	(2006.01)
A61B 18/00	(2006.01)

(52) **U.S. Cl.**

CPC ***A61F 9/00825*** (2013.01); *A61B 2018/00636* (2013.01); *A61F 2009/0087* (2013.01); *A61F 2009/00844* (2013.01); *A61F 2009/00889* (2013.01)

(58) **Field of Classification Search**

CPC A61F 2009/0087; A61F 9/008; A61F 2009/00851; A61F 2009/00889; A61F 9/00825; A61F 2009/00844; A61B 2018/00636

USPC 128/898; 606/4–6

See application file for complete search history.

(56) **References Cited**

U.S. PATENT DOCUMENTS

4,164,222	A	8/1979	Prokhorov et al.
4,198,143	A	4/1980	Karasawa
4,235,529	A	11/1980	Kawase et al.
4,465,348	A	8/1984	Lang
4,520,816	A	6/1985	Schachar et al.
4,533,222	A	8/1985	Ishikawa
4,538,608	A	9/1985	L'Esperance, Jr.
4,554,917	A	11/1985	Tagnon

(Continued)

FOREIGN PATENT DOCUMENTS

EP	1444946	8/2004
WO	98/08048	2/1998

(Continued)

OTHER PUBLICATIONS

Arimoto et al., "Imaging Properties of Axicon in a Scanning Optical System," Nov. 1, 1992, Applied Optics, 31 (31):6652-6657.

(Continued)

Primary Examiner — Gary Jackson
Assistant Examiner — Scott T Luan
(74) *Attorney, Agent, or Firm* — S. Brannon Latimer

(57) **ABSTRACT**

An imaging-based laser system can include a laser-beam system, configured to generate and scan a beam of laser pulses with an adjustable laser-power parameter to points of a scan-pattern in an eye, and an imaging-based laser-controller, configured to image a layer in the eye, to control the scanning of the beam of laser pulses to the points of the scan-pattern, and to control a laser-power parameter of the laser pulses according to the distance of the points of the scan-pattern from the imaged layer.

29 Claims, 26 Drawing Sheets

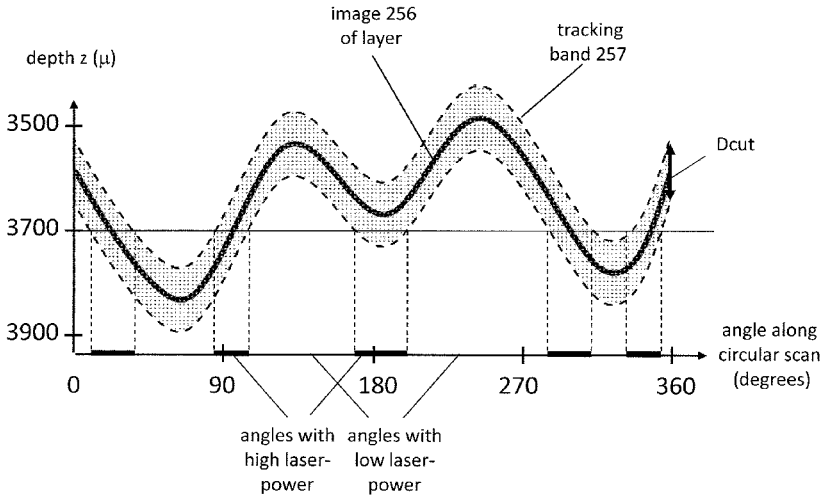

(56) **References Cited**

U.S. PATENT DOCUMENTS

4,638,801	A	1/1987	Daly et al.	
4,764,005	A	8/1988	Webb et al.	
4,881,808	A	11/1989	Bille et al.	
4,901,718	A	2/1990	Bille et al.	
4,907,586	A	3/1990	Bille et al.	
5,048,946	A	9/1991	Sklar et al.	
5,049,147	A	9/1991	Danon	
5,054,907	A	10/1991	Sklar et al.	
5,098,426	A	3/1992	Sklar et al.	
5,112,328	A	5/1992	Taboada et al.	
5,139,022	A	8/1992	Lempert	
5,246,435	A	9/1993	Bille et al.	
5,255,025	A	10/1993	Volk	
5,286,964	A	2/1994	Fountain	
5,321,501	A	6/1994	Swanson et al.	
5,336,215	A	8/1994	Hsueh et al.	
5,391,165	A	2/1995	Fountain et al.	
5,439,462	A	8/1995	Bille et al.	
5,493,109	A	2/1996	Wei et al.	
5,549,632	A	8/1996	Lai	
5,656,186	A	8/1997	Mouron et al.	
5,738,676	A	4/1998	Hammer et al.	
5,779,696	A	7/1998	Berry et al.	
5,795,295	A	8/1998	Hellmuth et al.	
5,936,706	A	8/1999	Takagi	
5,954,648	A	9/1999	Van Der Brug	
5,954,711	A	9/1999	Ozaki et al.	
5,994,690	A	11/1999	Kulkarni et al.	
6,004,314	A	12/1999	Wei et al.	
6,095,648	A	8/2000	Birngruber et al.	
6,099,522	A	8/2000	Knopp et al.	
6,137,585	A	10/2000	Hitzenberger et al.	
6,254,595	B1	7/2001	Juhasz et al.	
6,288,784	B1	9/2001	Hitzenberger et al.	
6,314,311	B1	11/2001	Williams et al.	
6,317,616	B1	11/2001	Glossop	
6,337,925	B1	1/2002	Cohen et al.	
6,377,349	B1	4/2002	Fercher	
6,379,005	B1	4/2002	Williams et al.	
6,451,009	B1	9/2002	Dasilva et al.	
6,454,761	B1	9/2002	Freedman	
6,497,701	B2	12/2002	Shimmick et al.	
6,529,758	B2	3/2003	Shahidi	
6,579,282	B2	6/2003	Bille et al.	
6,623,476	B2	9/2003	Juhasz et al.	
6,687,010	B1	2/2004	Horii et al.	
6,730,074	B2	5/2004	Bille et al.	
6,741,359	B2	5/2004	Wei et al.	
6,751,033	B2	6/2004	Goldstein et al.	
6,755,819	B1	6/2004	Waelti	
6,763,259	B1	7/2004	Hauger et al.	
6,769,769	B2	8/2004	Podoleanu et al.	
6,775,007	B2	8/2004	Izatt et al.	
6,863,667	B2	3/2005	Webb et al.	
6,887,232	B2	5/2005	Bille	
6,899,707	B2	5/2005	Scholler et al.	
6,932,807	B1	8/2005	Tomita et al.	
6,991,629	B1	1/2006	Juhasz et al.	
7,006,232	B2	2/2006	Rollins et al.	
7,018,376	B2	3/2006	Webb et al.	
7,027,233	B2	4/2006	Goldstein et al.	
7,061,622	B2	6/2006	Rollins et al.	
7,072,045	B2	7/2006	Chen et al.	
7,072,047	B2	7/2006	Westphal et al.	
7,079,254	B2	7/2006	Kane et al.	
7,102,756	B2	9/2006	Izatt et al.	
7,113,818	B2	9/2006	Podoleanu et al.	
7,126,693	B2	10/2006	Everett et al.	
7,130,054	B2	10/2006	Ostrovsky et al.	
7,133,137	B2	11/2006	Shimmick	
7,139,077	B2	11/2006	Podoleanu et al.	
7,145,661	B2	12/2006	Hitzenberger	
7,148,970	B2	12/2006	de Boer	
7,184,148	B2	2/2007	Alphonse	
7,207,983	B2	4/2007	Hahn et al.	
7,248,371	B2	7/2007	Chan et al.	
7,268,885	B2	9/2007	Chan et al.	
7,280,221	B2	10/2007	Wei	
7,307,733	B2	12/2007	Chan et al.	
7,310,150	B2	12/2007	Guillermo et al.	
7,312,876	B2	12/2007	Chan et al.	
7,319,566	B2	1/2008	Prince et al.	
7,329,002	B2	2/2008	Nakanishi	
7,330,270	B2	2/2008	O'Hara et al.	
7,330,273	B2	2/2008	Podoleanu et al.	
7,335,223	B2	2/2008	Obrebski	
7,336,366	B2	2/2008	Choma et al.	
7,342,659	B2	3/2008	Horn et al.	
7,347,548	B2	3/2008	Huang et al.	
7,352,444	B1	4/2008	Seams et al.	
7,355,716	B2	4/2008	de Boer et al.	
7,364,296	B2	4/2008	Miller et al.	
7,365,856	B2	4/2008	Everett et al.	
7,365,859	B2	4/2008	Yun et al.	
7,370,966	B2	5/2008	Fukuma et al.	
7,371,230	B2	5/2008	Webb et al.	
7,372,578	B2	5/2008	Akiba et al.	
7,388,672	B2	6/2008	Zhou et al.	
7,390,089	B2	6/2008	Loesel et al.	
7,400,410	B2	7/2008	Baker et al.	
7,402,159	B2	7/2008	Loesel et al.	
7,426,037	B2	9/2008	Ostrovsky et al.	
7,433,046	B2	10/2008	Everett et al.	
7,452,077	B2	11/2008	Meyer et al.	
7,452,080	B2	11/2008	Wiltberger et al.	
7,461,658	B2	12/2008	Jones et al.	
7,466,423	B2	12/2008	Podoleanu et al.	
7,470,025	B2	12/2008	Iwanaga	
7,477,764	B2	1/2009	Haisch	
7,480,058	B2	1/2009	Zhao et al.	
7,480,059	B2	1/2009	Zhou et al.	
7,488,070	B2	2/2009	Hauger et al.	
7,488,930	B2	2/2009	Ajgaonkar et al.	
7,492,466	B2	2/2009	Chan et al.	
7,503,916	B2	3/2009	Shimmick	
7,508,525	B2	3/2009	Zhou et al.	
7,535,577	B2	5/2009	Podoleanu et al.	
7,537,591	B2	5/2009	Feige et al.	
7,557,928	B2	7/2009	Ueno	
7,575,322	B2	8/2009	Somani	
7,593,559	B2	9/2009	Toth et al.	
7,602,500	B2	10/2009	Izatt et al.	
7,604,351	B2	10/2009	Fukuma et al.	
7,614,744	B2	11/2009	Abe	
7,630,083	B2	12/2009	de Boer et al.	
7,631,970	B2	12/2009	Wei	
7,633,627	B2	12/2009	Choma et al.	
7,643,152	B2	1/2010	de Boer et al.	
7,797,119	B2	9/2010	De Boer et al.	
7,813,644	B2	10/2010	Chen et al.	
7,898,712	B2	3/2011	Adams et al.	
8,262,646	B2	9/2012	Frey et al.	
8,382,745	B2 *	2/2013	Naranjo-Tackman et al.	606/5
8,394,084	B2 *	3/2013	Palankar et al.	606/6
2001/0022648	A1	9/2001	Lai	
2002/0013574	A1	1/2002	Elbrecht et al.	
2002/0082466	A1	6/2002	Han	
2002/0097374	A1	7/2002	Payne et al.	
2002/0133145	A1	9/2002	Gerlach et al.	
2002/0198516	A1	12/2002	Knopp	
2003/0090674	A1	5/2003	Zeylikovich et al.	
2003/0206272	A1	11/2003	Cornsweet et al.	
2004/0039378	A1	2/2004	Lin	
2004/0059321	A1	3/2004	Knopp et al.	
2004/0151466	A1	8/2004	Crossman-Bosworth et al.	
2004/0243233	A1	12/2004	Phillips	
2005/0010109	A1	1/2005	Faul	
2005/0015120	A1	1/2005	Seibel et al.	
2005/0021011	A1	1/2005	LaHaye	
2005/0173817	A1	8/2005	Fauver et al.	
2005/0192562	A1	9/2005	Loesel et al.	
2005/0201633	A1	9/2005	Moon et al.	
2005/0203492	A1	9/2005	Nguyen et al.	
2005/0215986	A1	9/2005	Chernyak et al.	

(56) **References Cited**

U.S. PATENT DOCUMENTS

2005/0284774	A1	12/2005	Mordaunt	
2005/0286019	A1	12/2005	Wiltberger et al.	
2005/0288745	A1	12/2005	Andersen et al.	
2006/0020172	A1	1/2006	Luerssen et al.	
2006/0077346	A1	4/2006	Matsumoto	
2006/0100613	A1	5/2006	McArdle et al.	
2006/0179992	A1	8/2006	Kermani	
2006/0187462	A1	8/2006	Srinivasan et al.	
2006/0195076	A1	8/2006	Blumenkranz et al.	
2006/0206102	A1	9/2006	Shimmick	
2007/0013867	A1	1/2007	Ichikawa	
2007/0121069	A1	5/2007	Andersen et al.	
2007/0126985	A1	6/2007	Wiltberger et al.	
2007/0129709	A1	6/2007	Andersen et al.	
2007/0129775	A1	6/2007	Mordaunt et al.	
2007/0147730	A1	6/2007	Wiltberger et al.	
2007/0173791	A1	7/2007	Raksi	
2007/0173794	A1	7/2007	Frey et al.	
2007/0173795	A1	7/2007	Frey et al.	
2007/0185475	A1	8/2007	Frey et al.	
2007/0189664	A1	8/2007	Andersen et al.	
2007/0216909	A1	9/2007	Everett et al.	
2007/0219541	A1	9/2007	Kurtz	
2007/0230520	A1	10/2007	Mordaunt et al.	
2007/0282313	A1	12/2007	Huang et al.	
2007/0291277	A1	12/2007	Everett et al.	
2007/0299429	A1	12/2007	Amano	
2008/0033406	A1	2/2008	Andersen et al.	
2008/0049188	A1	2/2008	Wiltberger et al.	
2008/0055543	A1	3/2008	Meyer et al.	
2008/0056610	A1	3/2008	Kanda	
2008/0071254	A1	3/2008	Lummis et al.	
2008/0088795	A1	4/2008	Goldstein et al.	
2008/0100612	A1	5/2008	Dastmalchi et al.	
2008/0281303	A1	11/2008	Culbertson et al.	
2008/0281413	A1	11/2008	Culbertson et al.	
2008/0319427	A1	12/2008	Palanker	
2009/0012507	A1	1/2009	Culbertson et al.	
2009/0088734	A1	4/2009	Mordaunt	
2009/0125005	A1	5/2009	Chernyak et al.	
2009/0131921	A1	5/2009	Kurtz et al.	
2009/0149742	A1	6/2009	Kato et al.	
2009/0157062	A1	6/2009	Hauger et al.	
2009/0161827	A1	6/2009	Gertner et al.	
2009/0168017	A1	7/2009	O'Hara et al.	
2009/0177189	A1	7/2009	Raksi	
2009/0268161	A1	10/2009	Hart et al.	
2010/0004641	A1	1/2010	Frey et al.	
2010/0004643	A1	1/2010	Frey et al.	
2010/0007848	A1	1/2010	Murata	
2010/0022994	A1	1/2010	Frey et al.	
2010/0022995	A1	1/2010	Frey et al.	
2010/0022996	A1	1/2010	Frey et al.	
2010/0042079	A1	2/2010	Frey et al.	
2010/0110377	A1	5/2010	Maloca et al.	
2010/0137850	A1*	6/2010	Culbertson et al.	606/6
2010/0292678	A1*	11/2010	Frey et al.	606/5
2010/0324543	A1	12/2010	Kurtz et al.	
2011/0022036	A1	1/2011	Frey et al.	
2011/0106066	A1*	5/2011	Bor	606/5
2011/0118609	A1	5/2011	Goldshleger et al.	
2011/0166557	A1*	7/2011	Naranjo-Tackman et al.	606/5
2011/0184392	A1*	7/2011	Culbertson et al.	606/4
2011/0184395	A1*	7/2011	Schuele et al.	606/5
2011/0196350	A1*	8/2011	Friedman et al.	606/6
2011/0202046	A1*	8/2011	Angeley et al.	606/6
2011/0319873	A1	12/2011	Raksi et al.	
2012/0089134	A1*	4/2012	Horvath et al.	606/6
2012/0274903	A1	11/2012	Sayeram et al.	

FOREIGN PATENT DOCUMENTS

WO	03/062802	7/2003
WO	2006074469	7/2006
WO	2007/084694	7/2007
WO	2007106326	9/2007
WO	2007/130411	11/2007
WO	2010/075571	7/2010
WO	2011/011788	1/2011

OTHER PUBLICATIONS

Birngruber et al., "In-Vivo Imaging of the Development of Linear and Non-Linear Retinal Laser Effects Using Optical Coherence Tomography in Correlation with Histopathological Findings," 1995, Proc. SPIE 2391:21-27.

Chinn, S.R., et al., "Optical coherence tomography using a frequency-tunable optical source", Optics Letters, 22 (5):340-342, Mar. 1997.

European Search Report, European Patent Application No. 10191057.8, mailed Mar. 16, 2011, to be published by the USPTO.

Fercher et al., "Eye-Length Measurement by Interferometry With Partially Coherent Light," Mar. 1988, Optics Letters, 13(3):186-188.

Fercher et al., "Measurement of Intraocular Distances by Backscattering Spectral Interferometry," May 15, 1995, Optics Comm. 117:43-48.

Hee, M., et al., "Femotosecond transillumination optical coherence tomography", Optics Letters, 18(12):950-952, Jun. 1993.

Huber, R., et al., "Three-dimensional and C-mode OCT imaging with a compact, frequency swept laser source at 1300 nm", Optics Express, 13(26):10523-10538, Dec. 2005.

Izatt et al., "Micron-Resolution Biomedical Imaging With Optical Coherence Tomography," Oct. 1993, Optics & Photonics News, pp. 14-19.

Kamensky, V., et al., "In situ monitoring of the middle IR laser ablation of a cataract-suffered human lens by optical coherent tomography", Proc. SPIE, 2930:222-229, 1996.

Kamensky, V., et al., "Monitoring and animation of laser ablation process in cataracted eye lens using coherence tomography", Proc. SPIE, 2981:94-102, 1997.

Massow, O., et al., "Optical coherence tomography controlled femtosecond laser microsurgery system", Proceedings of the SPIE—Optical Coherence Tomography and Coherence Techniques III, vol. 6627, pp. 662717(1)-662717(6), Aug. 2007.

Ohmi, M., et al., "In-situ Observation of Tissue Laser Ablation Using Optical Coherence Tomography", Optical and Quantum Electronics, 37(13-15):1175-1183, Dec. 2005.

Ostaszewski et al., "Risley prism Beam Pointer", Proc. of SPIE, vol. 6304, 630406-1 thru 630406-10.

PCT International Search Report for International Application No. PCT/US2011/023710 mailed Aug. 24, 2011.

PCT International Search Report for International Application No. PCT/US2011/025332 mailed Sep. 16, 2011.

PCT International Search Report for International Application No. PCT/US2010/056701 mailed Jan. 12, 2011.

PCT International Search Report for International Application No. PCT/US2008/075511 mailed Mar. 12, 2009.

Sarunic, M., et al., "Instantaneous complex conjugate resolved spectral domain and swept-source OCT using 3×3 fiber couplers", Optics Express, 13(3):957-967, Feb. 2005.

Sarunic, M., et al., "Real-time quadrature projection complex conjugate resolved Fourier domain optical coherence tomography", Optics Letters, 31(16):2426-2428, Aug. 2006.

Sarunic, M., et al., "Imaging the Ocular Anterior Segment With Real-Time, Full-Range Fourier-Domain Optical Coherence Tomography", Archives of Ophthalmology, 126(4):537-542, Apr. 2008.

Stern et al., "Femtosecond Optical Ranging of Corneal Incision Depth," Jan. 1989, Investigative Ophthalmology & Visual Science, 30(1):99-104.

Swanson et al., "In vivo retinal imaging by optical coherence tomography", Optics Letters, 18(21), 1864-1866, Nov. 1993.

Tao, Y., et al., "High-speed complex conjugate resolved retinal spectral domain optical coherence tomography using sinusoidal phase modulation", Optics letters, 32(20):2918-2920, Oct. 2007.

(56) **References Cited**

OTHER PUBLICATIONS

Wojtkowski et al., "In Vivo Human Retinal Imaging by Fourier Domain Optical Coherence Tomography," Jul. 2002, Journal of Biomedical Optics 7(3):457-463, 7 pages.
Yun, S.H., et al., "Wavelength-swept fiber laser with frequency shifted feedback and resonantly swept intra-cavity acoustooptic tunable filter", IEEE Journal of Selected Topics in Quantum Electronics, 3(4):1087-1096, Aug. 1997.
PCT International Search Report corresponding to PCT Application Serial No. PCT/US2011/051466 dated Apr. 10, 2012.
Partial International Search Report corresponding to PCT Application Serial No. PCT/US2012/035927 dated Aug. 3, 2012.
PCT International Search Report dated Jun. 29, 2012 for International Application No. PCT/US2011/051360, filed Sep. 13, 2011.
PCT International Search Report and Written Opinion dated Feb. 9, 2012 for International Application Serial No. PCT/US2011/040223.
Aslyo-Vogel et al., "Darstellung von LTK-Läsionen durch optische Kurzkohärenztomographie (OCT) und Polarisationsmikroskopie nach Sirius-Rot-Fäbung", Ophthalmologe, pp. 487-491, 7-97.
Bagayev et al., "Optical coherence tomography for in situ monitoring of laser corneal ablation", Journal of Biomedical Optics, 7(4), pp. 633-642 (Oct. 2002).
Blaha et al., "The slit lamp and the laser in ophthalmology—a new laser slit lamp", SPIE Optical Instrumentation for Biomedical Laser Applications, vol. 658, pp. 38-42, 1986.
Boppart, S., et al., "Intraoperative Assessment of Microsurgery with Three-dimensional Optical Coherence Tomography", Radiology, 208(1):81-86, Jul. 1998.
Davidson, "Analytic Waveguide Solutions and the Coherence Probe Microscope", Microelectronic Engineering, 13, pp. 523-526, 1991.
Drexler, W., et al., "Measurement of the thickness of fundus layers by partial coherence tomography", Optical Engineering, 34(3):701-710, Mar. 1995.
Dyer, R, et al., "Optical Fibre Delivery and Tissue Ablation Studies using a Pulsed Hydrogen Fluoride Laser", Lasers in Medical Science, 7:331-340, 1992.
Fercher et al., "In Vivo Optical Coherence Tomography", American Journal of Ophthalmology, 116(1), pp. 113-114, 1993.
Fujimoto, J., et al., :Biomedical Imaging using Optical Coherent Tomography, 1994, 67.
Hammer, D., "Ultrashort pulse laser induced bubble creation thresholds in ocular media", SPIE, 2391:30-40, 1995.
Hauger, C., et al., "High speed low coherence interferometer for optical coherence tomography", Proceedings of SPIE, 4619:1-9, 2002.
Hee, M., et al., "Optical Coherence tomography of the Human Retina", Arch Ophthalmol, 113:325-332; Mar. 1995.
Hitzenberger et al., "Interferometric Measurement of Corneal Thickness With Micrometer Precision", American Journal of Ophthalmology, 118:468-476, Oct. 1994.
Hitzenberger, C., et al., "Retinal layers located with a precision of 5 μm by partial coherence interferometry", SPIE, 2393:176-181, 1995.
Itoh et al., "Absolute measurements of 3-D shape using white-light interferometer", SPIE Interferometry: Techniques and Analysis, 1755:24-28, 1992.
Izatt et al., "Ophthalmic Diagnostics using Optical Coherence Tomography", SPIE Ophthalmic Technologies, 1877:136-144, 1993.
Izatt, J., et al., "Micrometer-Scale Resolution Imaging of the Anterior Eye In vivo With Optical Coherence Tomography", Arch Ophthalmol, 112:1584-1589, Dec. 1994.
Jean, B., et al., "Topography assisted photoablation", SPIE, vol. 3591:202-208, 1999.
Kamensky, V., et al., "In Situ Monitoring of Laser Modification Process in Human Cataractous Lens and Porcine Cornea Using Coherence Tomography", Journal of biomedical Optics, 4(1), 137-143, Jan. 1999.
Lee et al., "Profilometry with a coherence scanning microscope", Applied Optics, 29(26), 3784-3788, Sep. 10, 1990.
Lubatschowski, "The German Ministry of Research and education funded this OCT guided fs laser surgery in Sep. 2005", http://www.laser-zentrum-hannover.de/download/pdf/taetigkeitsbericht2005.pdf.
Massow, O., et al., "Femotosecond laser microsurgery system controlled by OCT", Laser Zentrum Hannover e.V., The German Ministry of education and research,19 slides, 2007.
Puliafito, Carmen, "Final technical Report: Air Force Grant #F49620-93-I-03337(1)" dated Feb. 12, 1997, 9 pages.
Ren, Q., et al., "Axicon: A New Laser Beam Delivery System for Corneal Surgery", IEEE Journal of Quantum Electronics, 26(12):2305-2308, Dec. 1990.
Ren, Q., et al., "Cataract Surgery with a Mid-Infrared Endo-laser System", SPIE Ophthalmic Technologies II, 1644:188-192, 1992.
Thompson, K., et al., "Therapeutic and Diagnostic Application of Lasers in Ophthalmology", Proceedings of the IEEE, 80(6):838-860, Jun. 1992.
Thrane, L, et al., "Calculation of the maximum obtainable probing depth of optical coherence tomography in tissue", Proceedings of SPIE, 3915:2-11, 2000.
Wisweh, H., et al., "OCT controlled vocal fold femtosecond laser microsurgery", Laser Zentrum Hannover e.V., The German Ministry of education and research, Grants: 13N8710 and 13N8712; 23 slides, 2008.

* cited by examiner

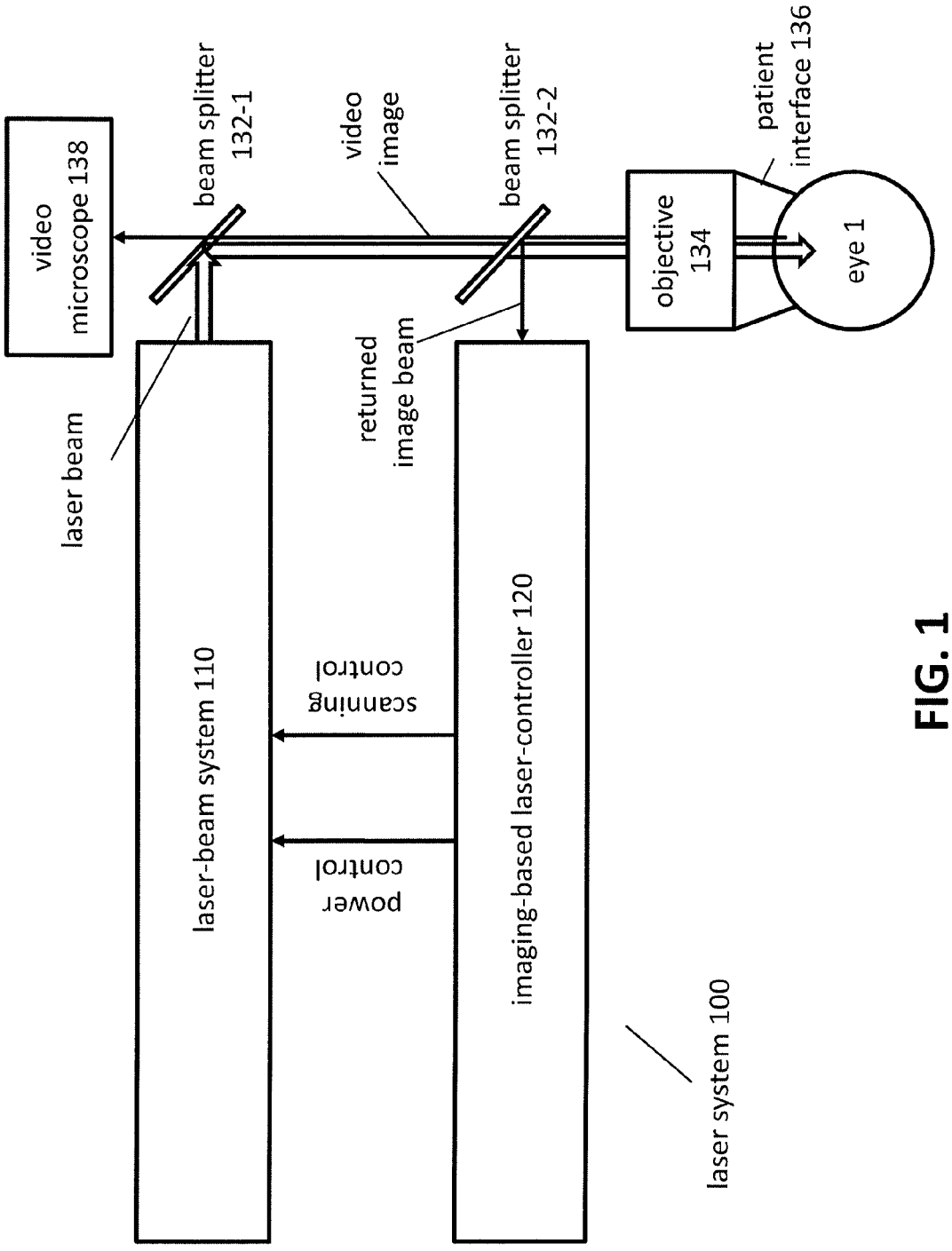
video microscope 138
beam splitter 132-1
video image
beam splitter 132-2
patient interface 136
objective 134
eye 1
laser beam
returned image beam
laser-beam system 110
scanning control
power control
imaging-based laser-controller 120
laser system 100

FIG. 1

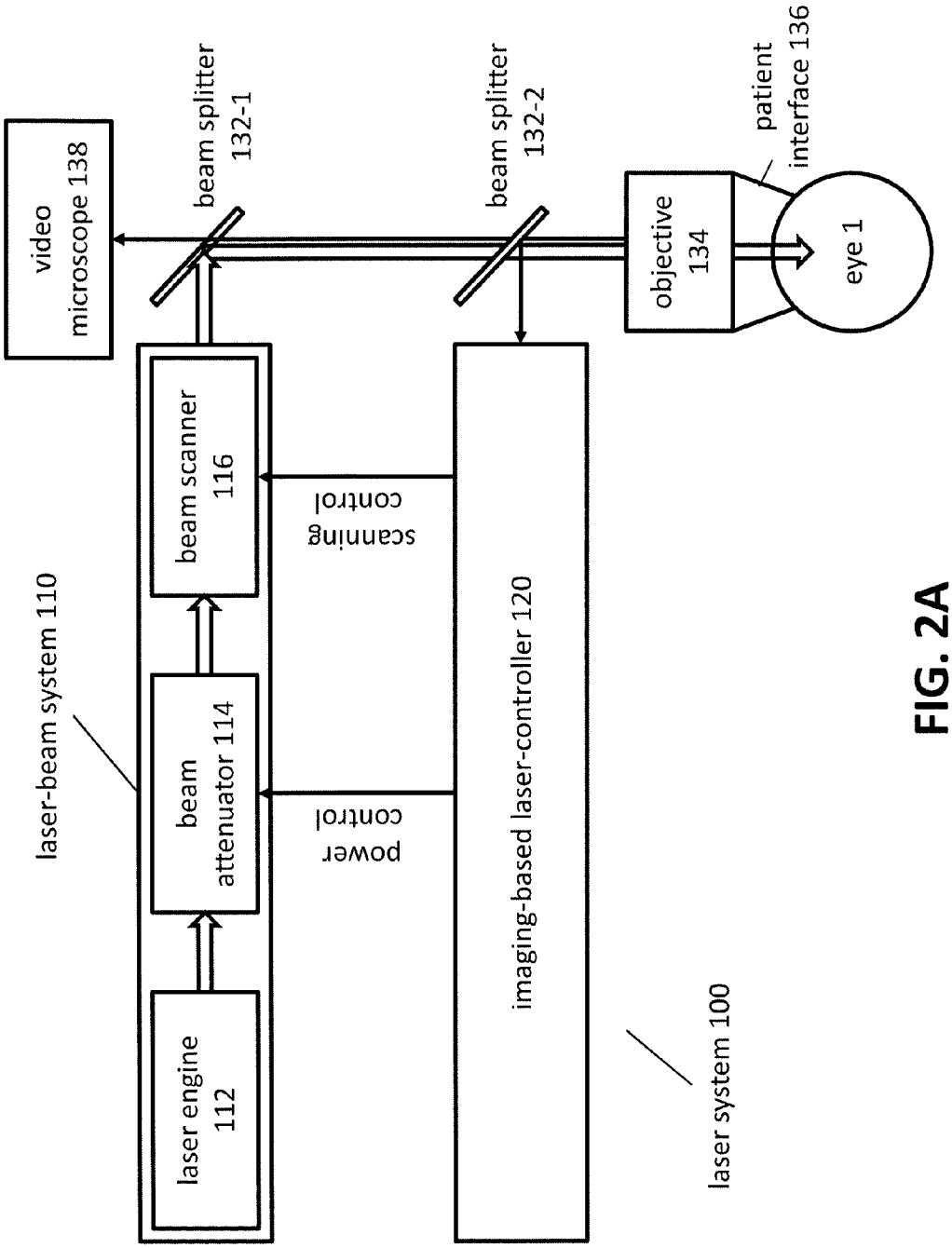
video microscope 138
beam splitter 132-1
beam splitter 132-2
patient interface 136
objective 134
eye 1
beam scanner 116
scanning control
beam attenuator 114
power control
laser engine 112
laser-beam system 110
imaging-based laser-controller 120
laser system 100

FIG. 2A

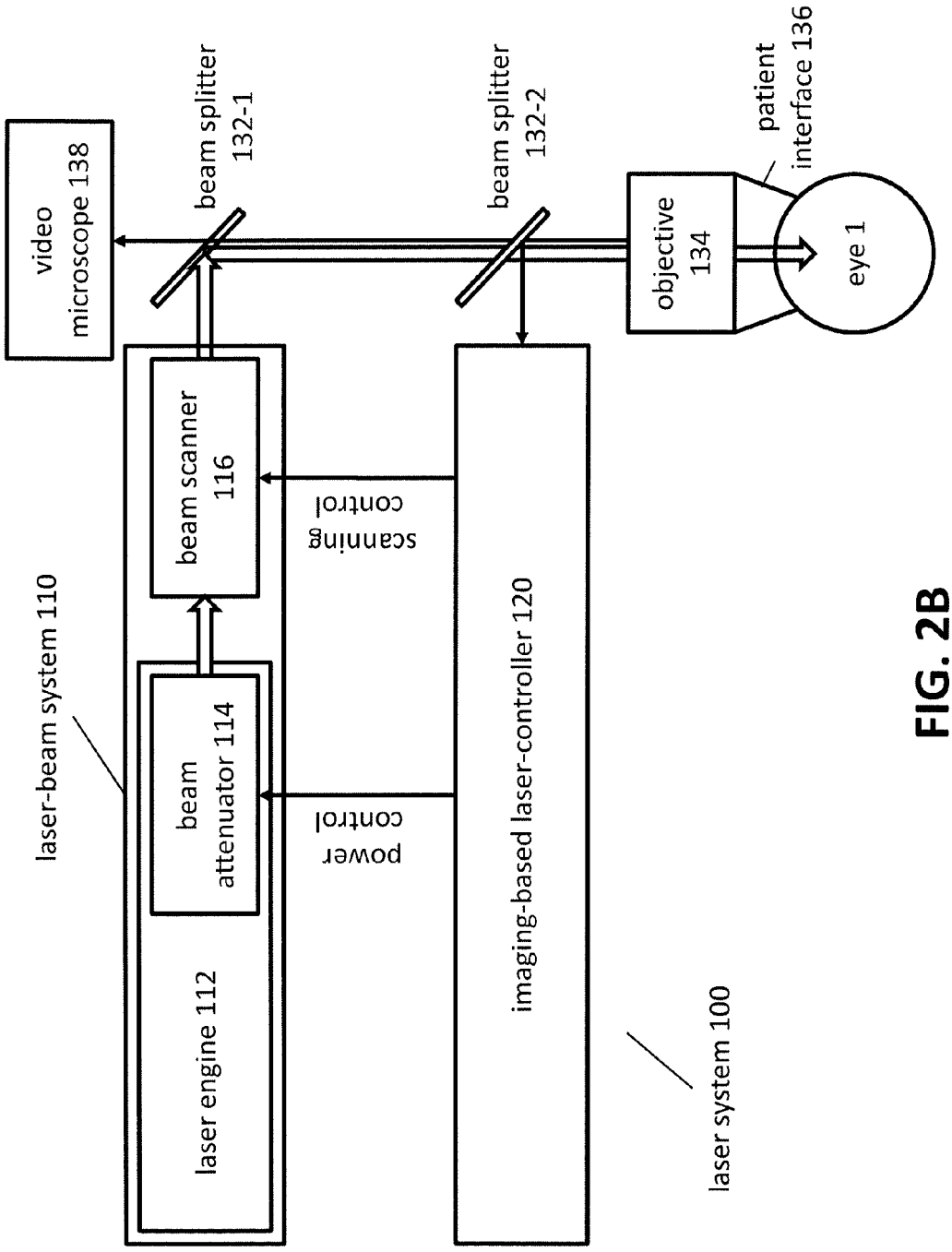
video microscope 138
beam splitter 132-1
beam splitter 132-2
patient interface 136
objective 134
eye 1
beam scanner 116
scanning control
beam attenuator 114
power control
laser-beam system 110
laser engine 112
imaging-based laser-controller 120
laser system 100

FIG. 2B

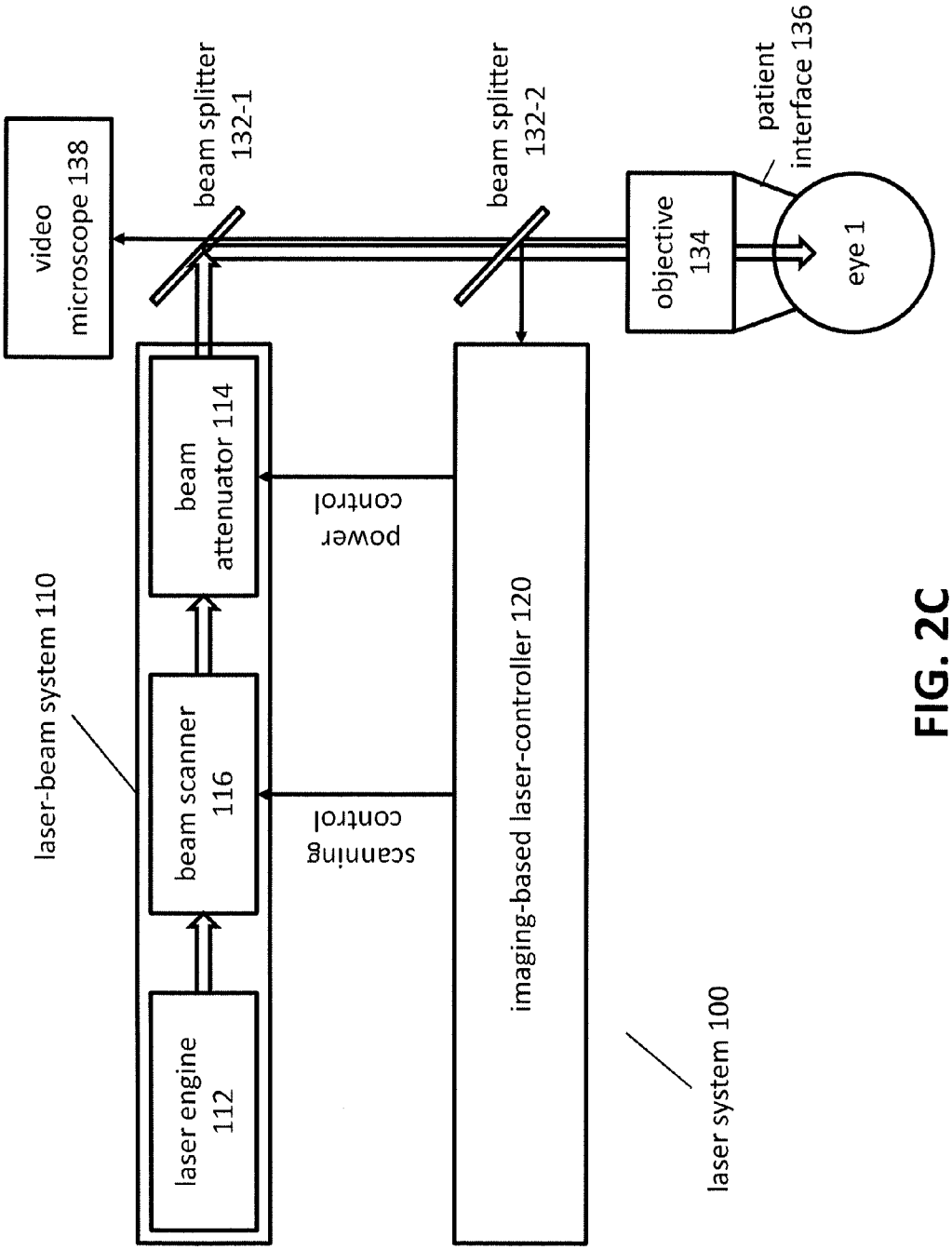
video microscope 138
beam splitter 132-1
beam splitter 132-2
patient interface 136
objective 134
eye 1
beam attenuator 114
power control
imaging-based laser-controller 120
laser-beam system 110
beam scanner 116
scanning control
laser engine 112
laser system 100

FIG. 2C

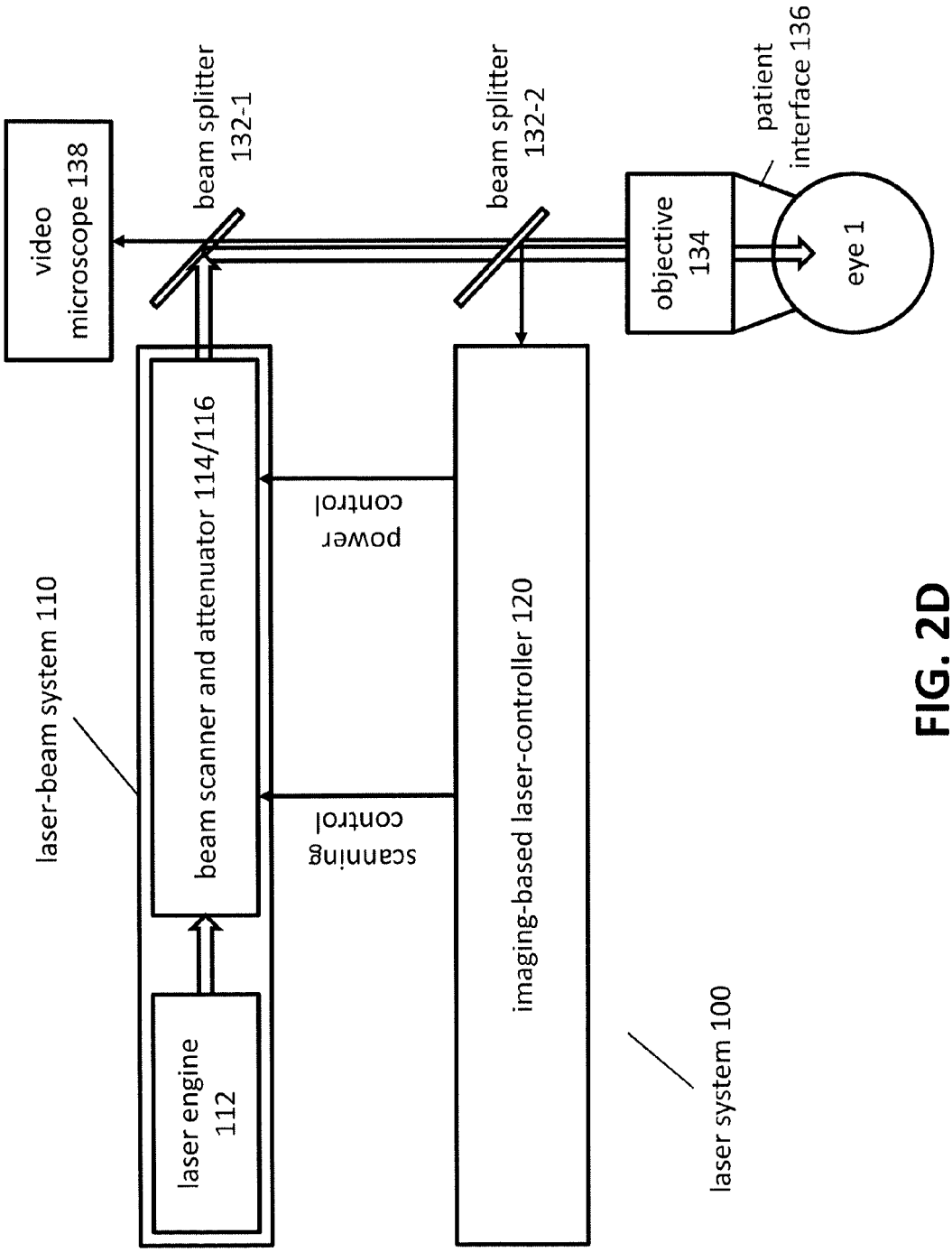
video microscope 138
beam splitter 132-1
beam splitter 132-2
patient interface 136
objective 134
eye 1
beam scanner and attenuator 114/116
power control
scanning control
imaging-based laser-controller 120
laser-beam system 110
laser engine 112
laser system 100

FIG. 2D

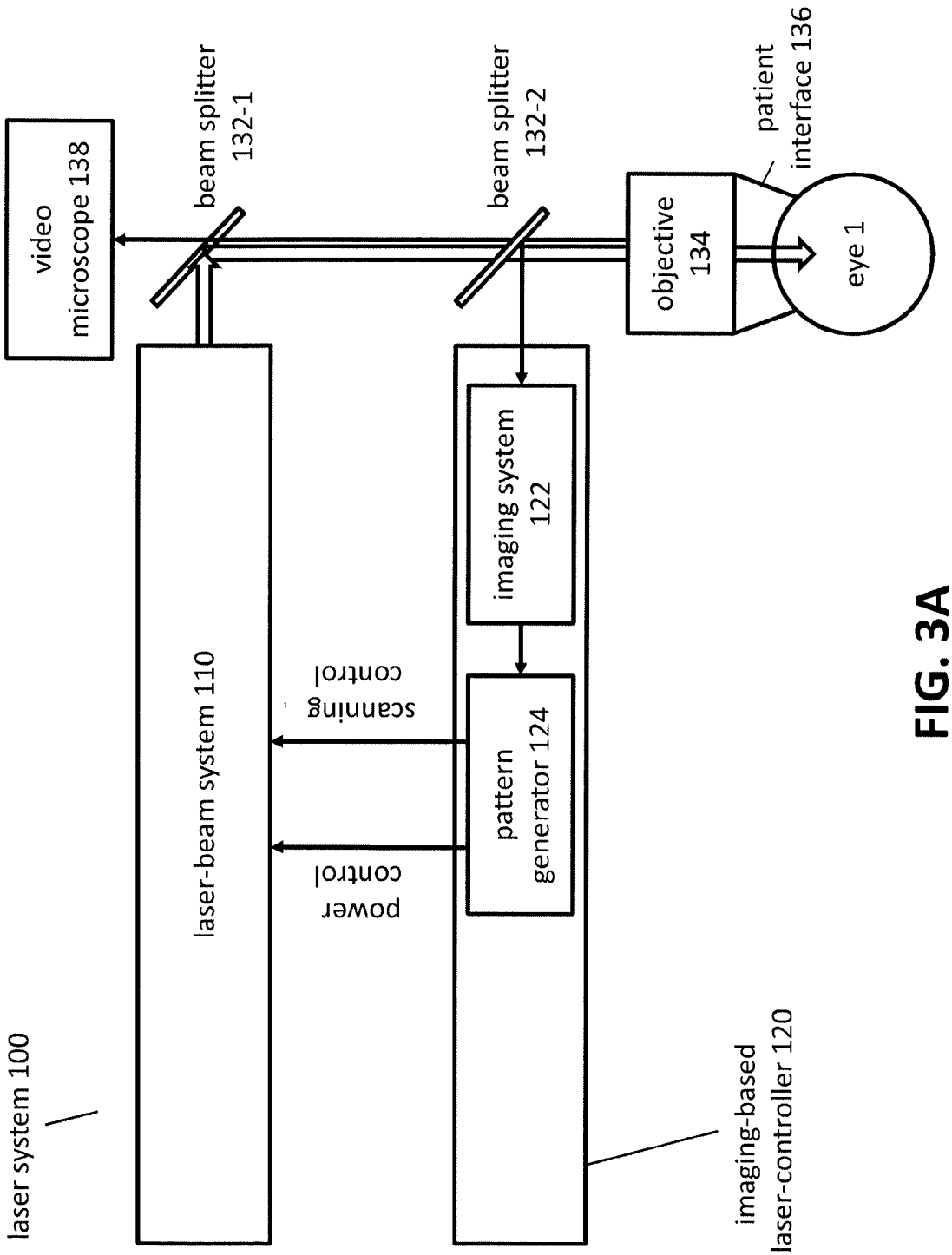
video microscope 138
beam splitter 132-1
beam splitter 132-2
patient interface 136
objective 134
eye 1
imaging system 122
pattern generator 124
scanning control
power control
laser-beam system 110
laser system 100
imaging-based laser-controller 120

FIG. 3A

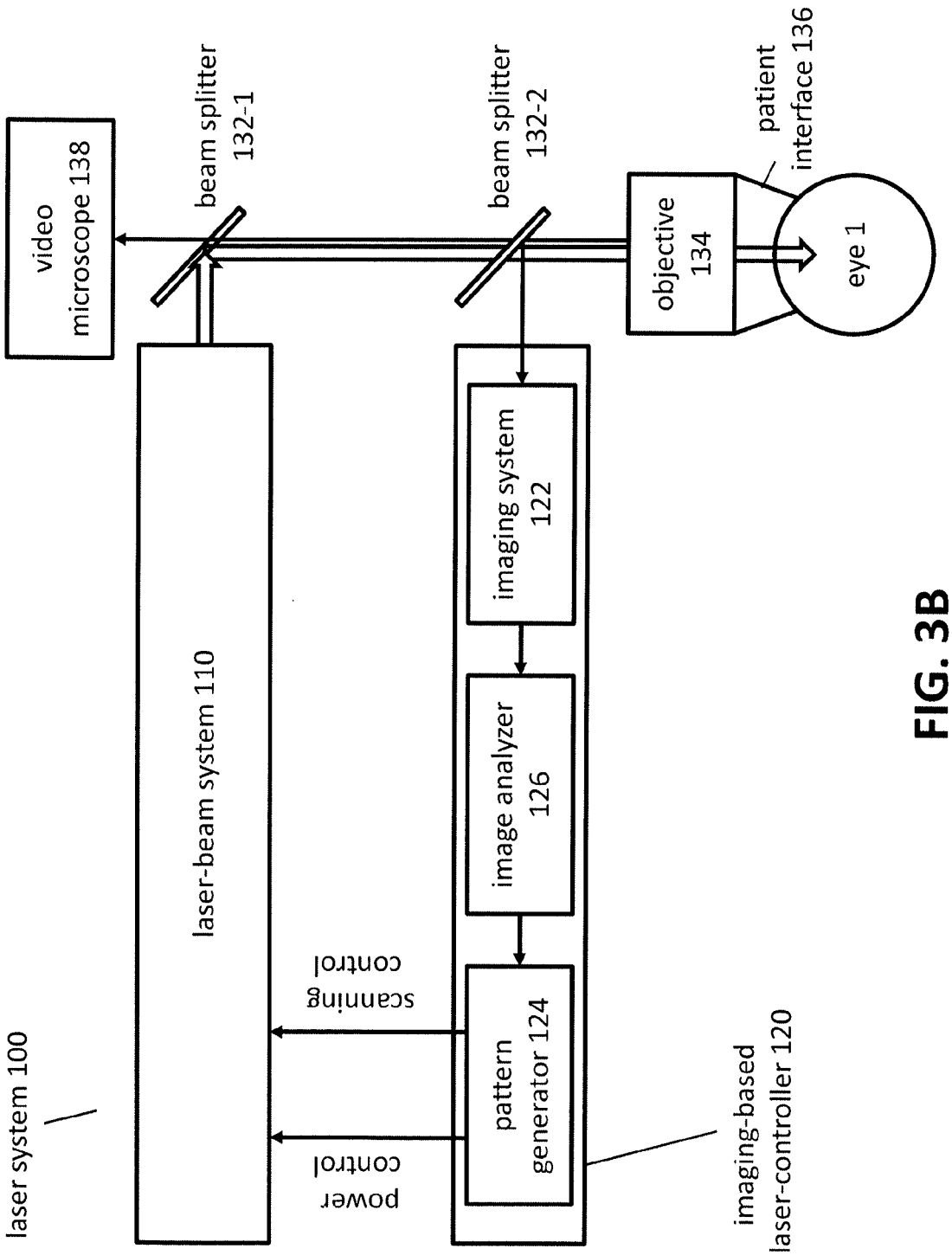
video microscope 138
beam splitter 132-1
beam splitter 132-2
patient interface 136
objective 134
eye 1
imaging system 122
image analyzer 126
pattern generator 124
laser-beam system 110
scanning control
power control
laser system 100
imaging-based laser-controller 120

FIG. 3B

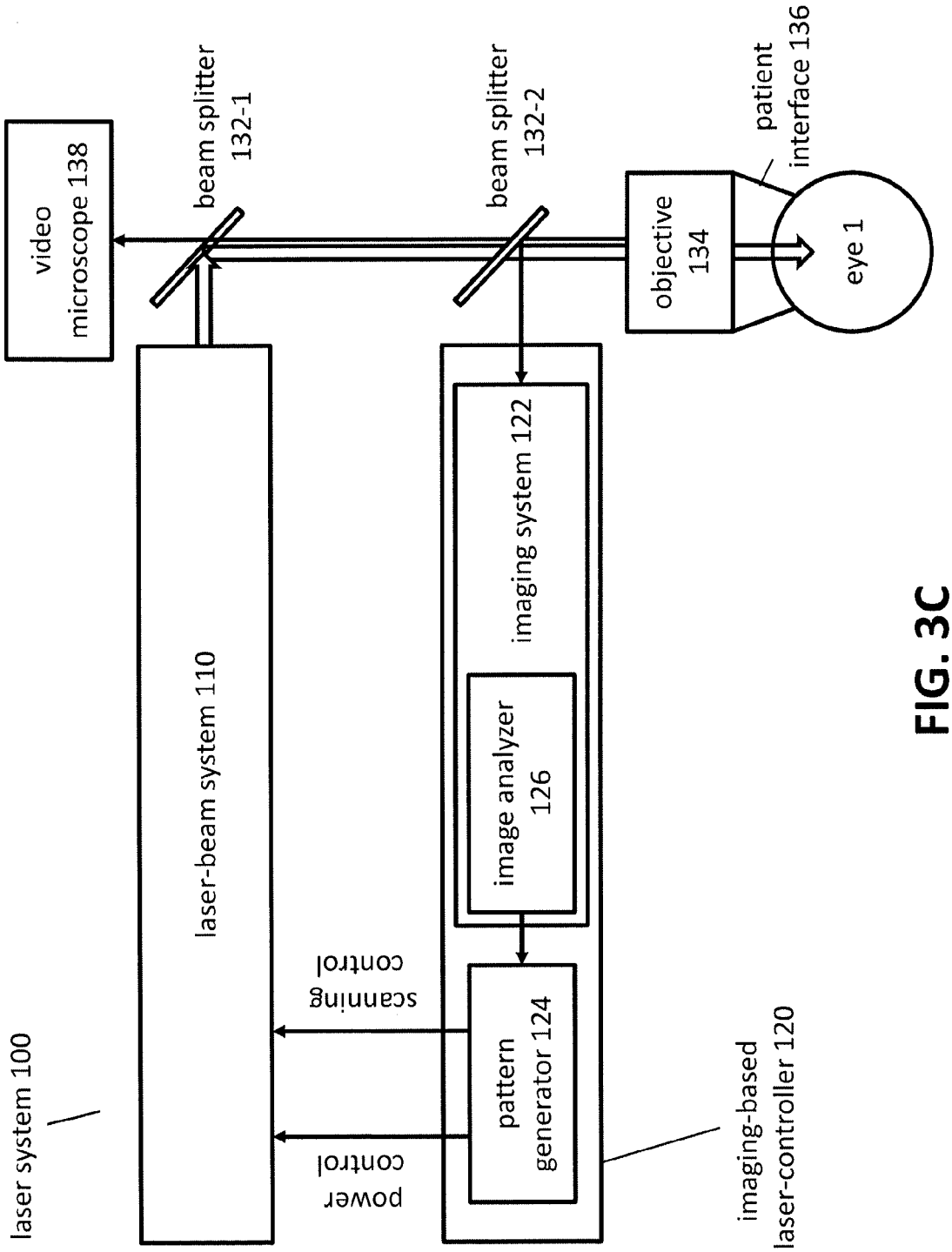
video microscope 138
beam splitter 132-1
beam splitter 132-2
patient interface 136
objective 134
eye 1
laser-beam system 110
imaging system 122
image analyzer 126
pattern generator 124
scanning control
power control
laser system 100
imaging-based laser-controller 120

FIG. 3C

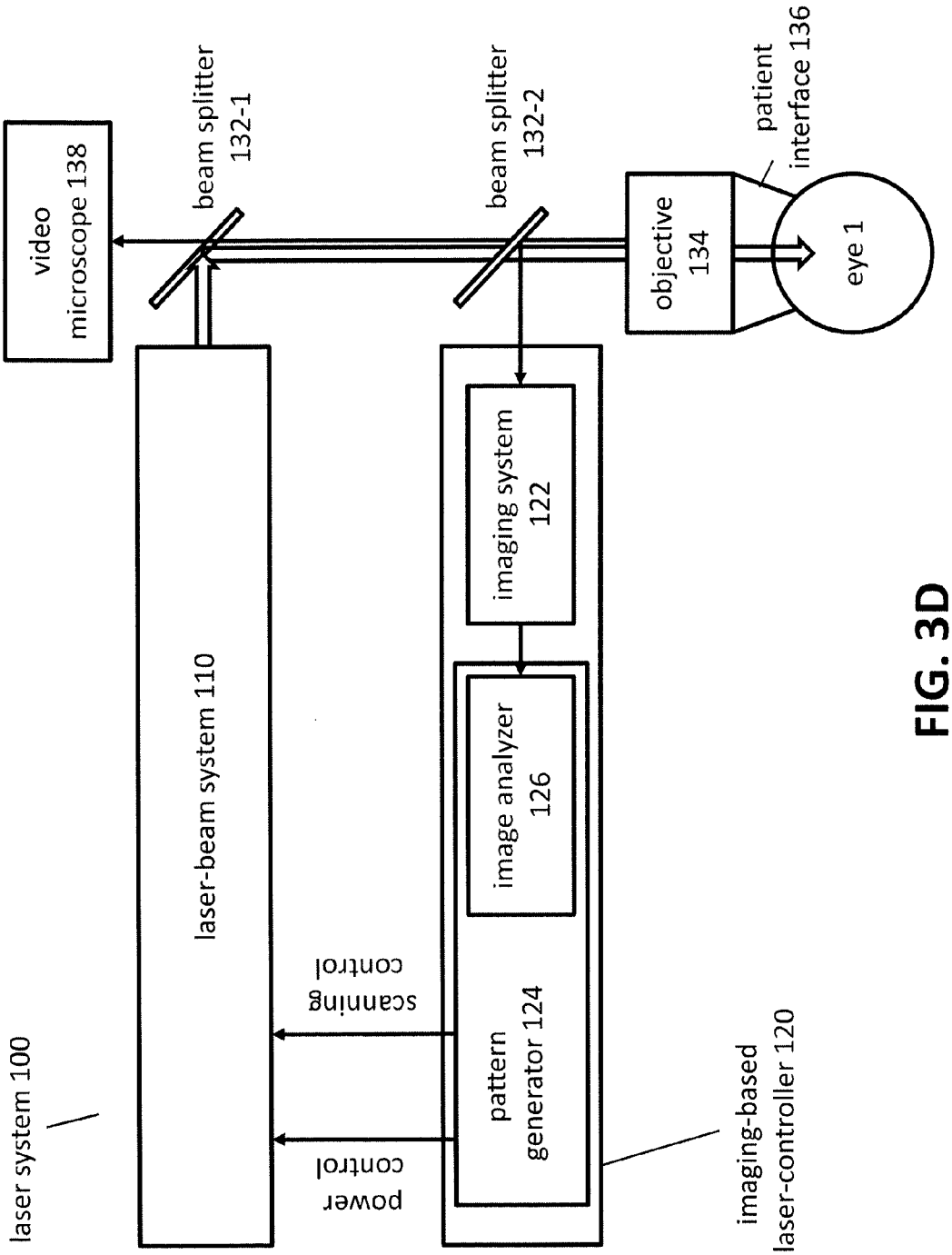
video microscope 138
beam splitter 132-1
beam splitter 132-2
patient interface 136
objective 134
eye 1
imaging system 122
image analyzer 126
pattern generator 124
laser-beam system 110
scanning control
power control
laser system 100
imaging-based laser-controller 120

FIG. 3D

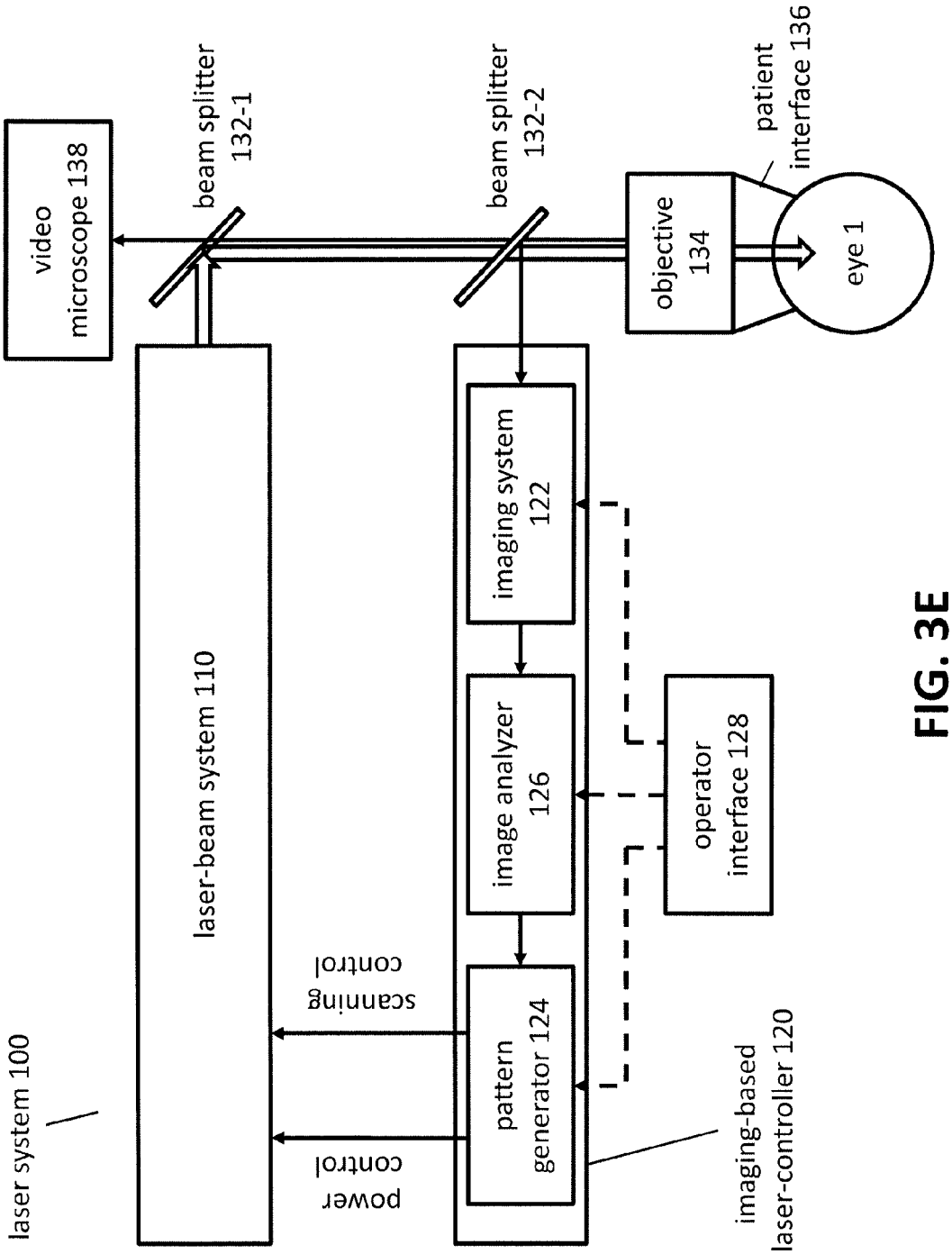
video microscope 138
beam splitter 132-1
beam splitter 132-2
patient interface 136
objective 134
eye 1
laser-beam system 110
imaging system 122
image analyzer 126
operator interface 128
pattern generator 124
scanning control
power control
laser system 100
imaging-based laser-controller 120

FIG. 3E

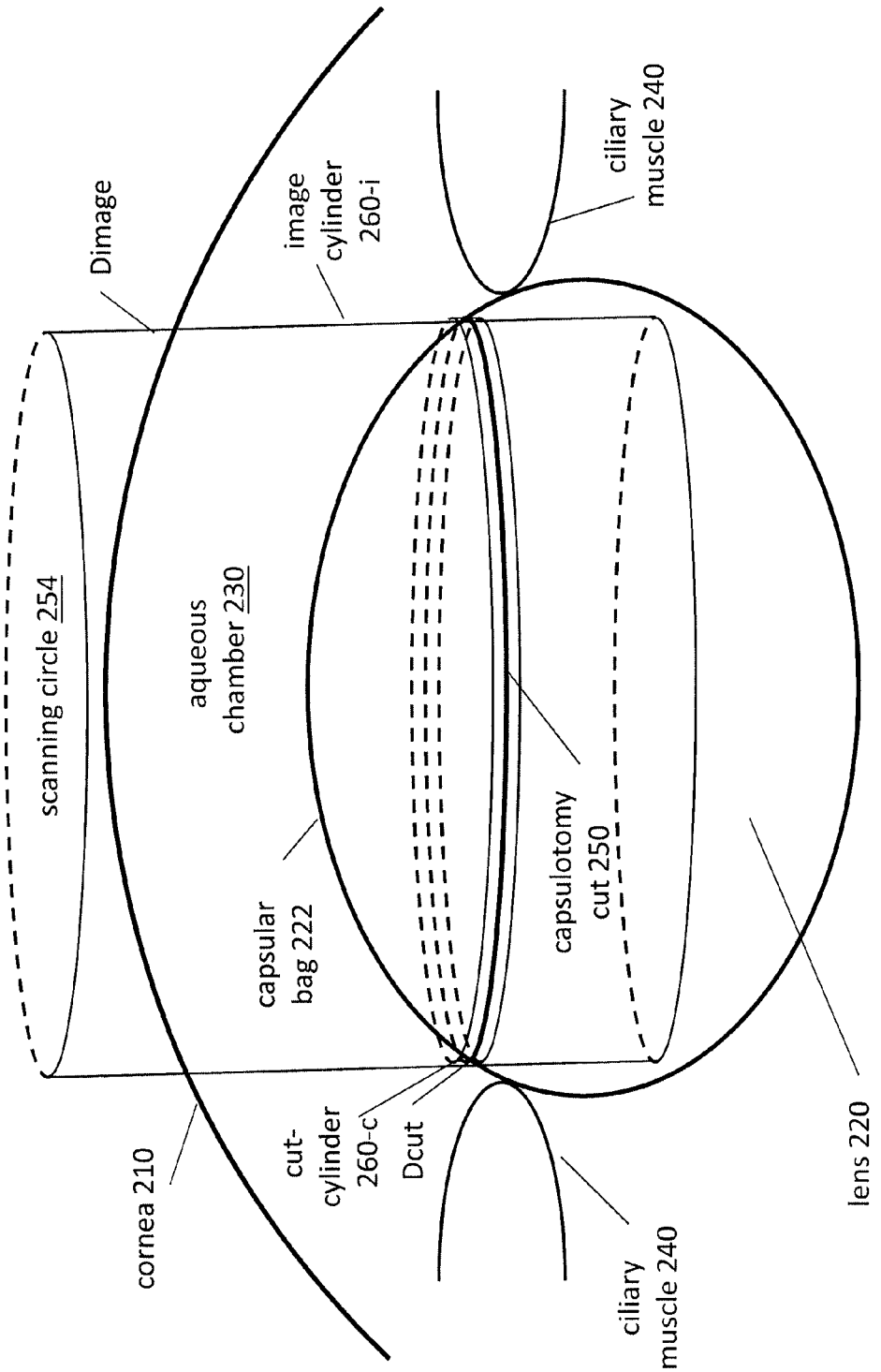
Dimage
image cylinder 260-i
ciliary muscle 240
scanning circle 254
aqueous chamber 230
capsular bag 222
capsulotomy cut 250
cornea 210
cut-cylinder 260-c
Dcut
ciliary muscle 240
lens 220

FIG. 4A

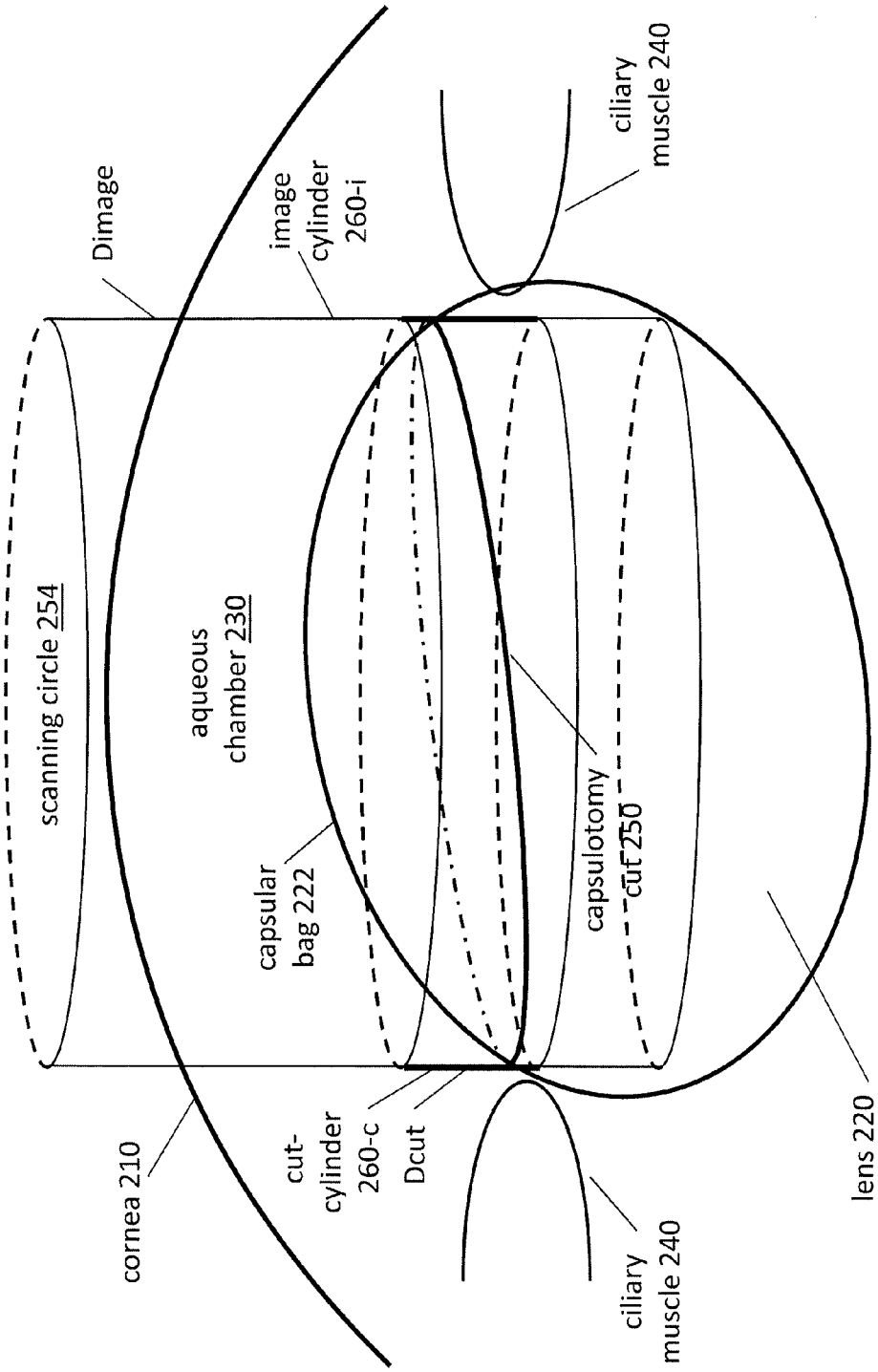
Dimage
image cylinder 260-i
ciliary muscle 240
scanning circle 254
aqueous chamber 230
capsular bag 222
capsulotomy cut 250
cornea 210
cut-cylinder 260-c
Dcut
ciliary muscle 240
lens 220

FIG. 4B

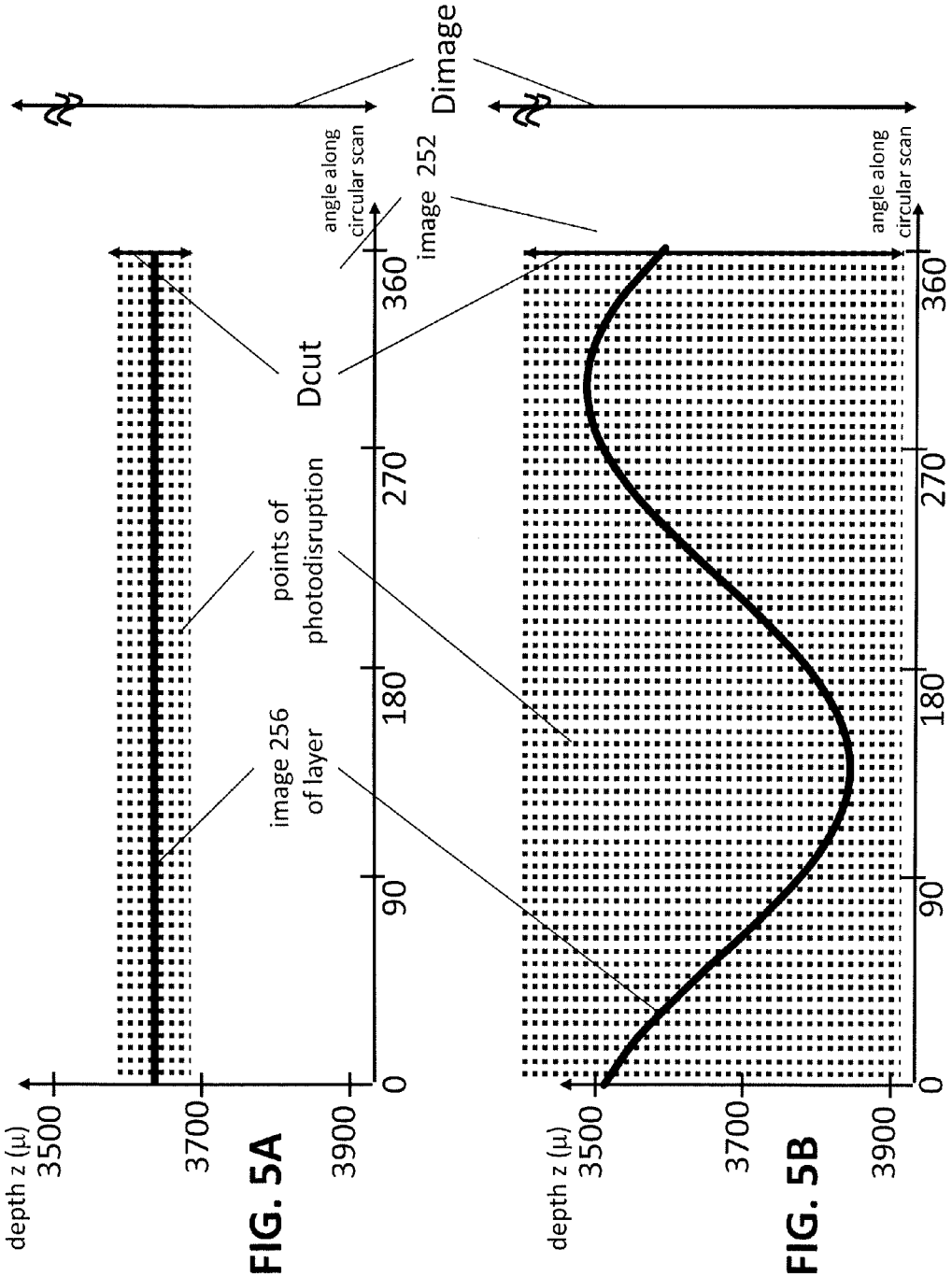
Dimage
Dcut
image 252
image 256 of layer
points of photodisruption
angle along circular scan
depth z (μ)
3500
3700
3900
0
90
180
270
360

FIG. 5A

FIG. 5B

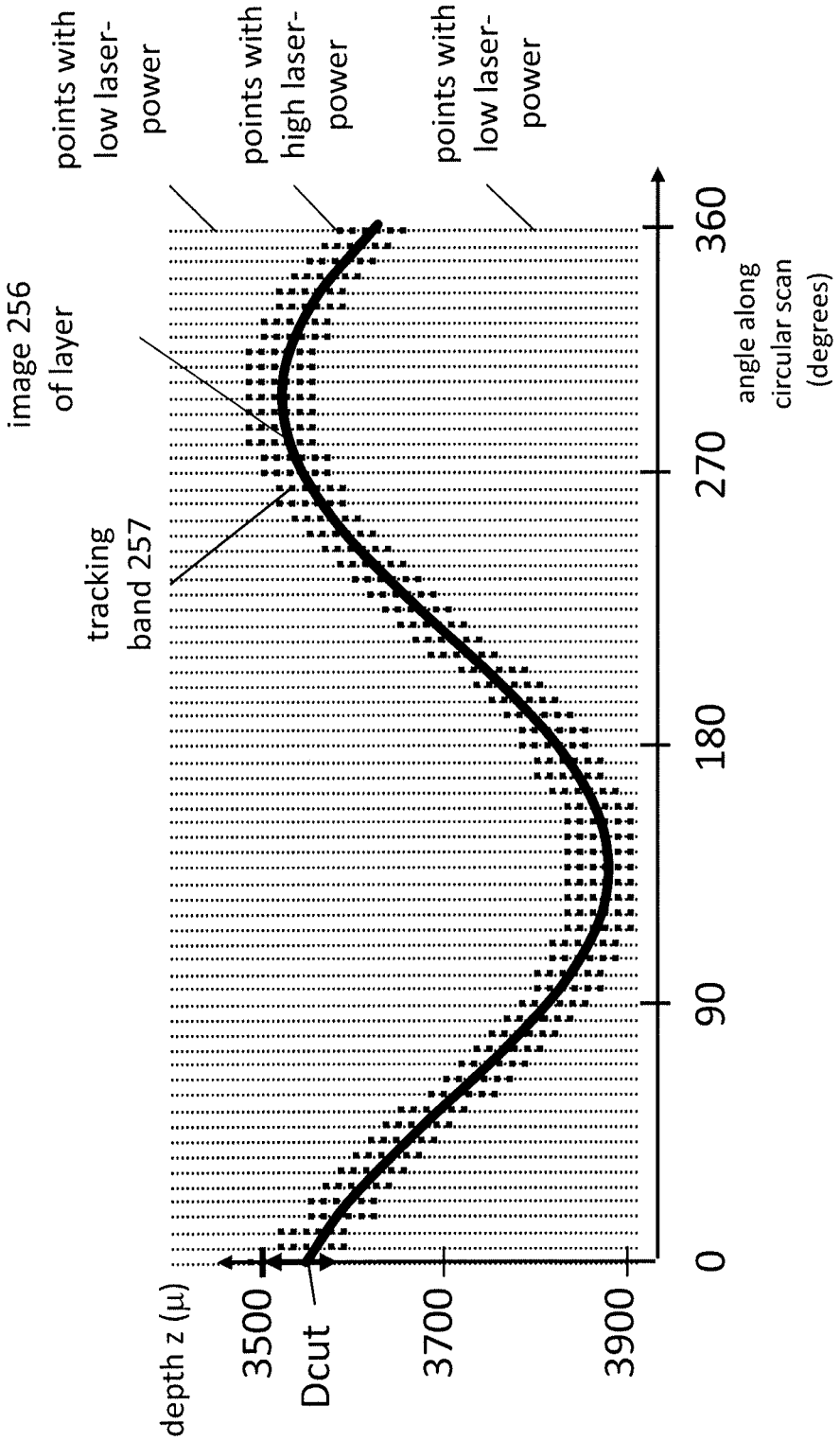
points with low laser-power
points with high laser-power
points with low laser-power
image 256 of layer
tracking band 257
depth z (μ)
3500
Dcut
3700
3900
0
90
180
270
360
angle along circular scan (degrees)

FIG. 6A

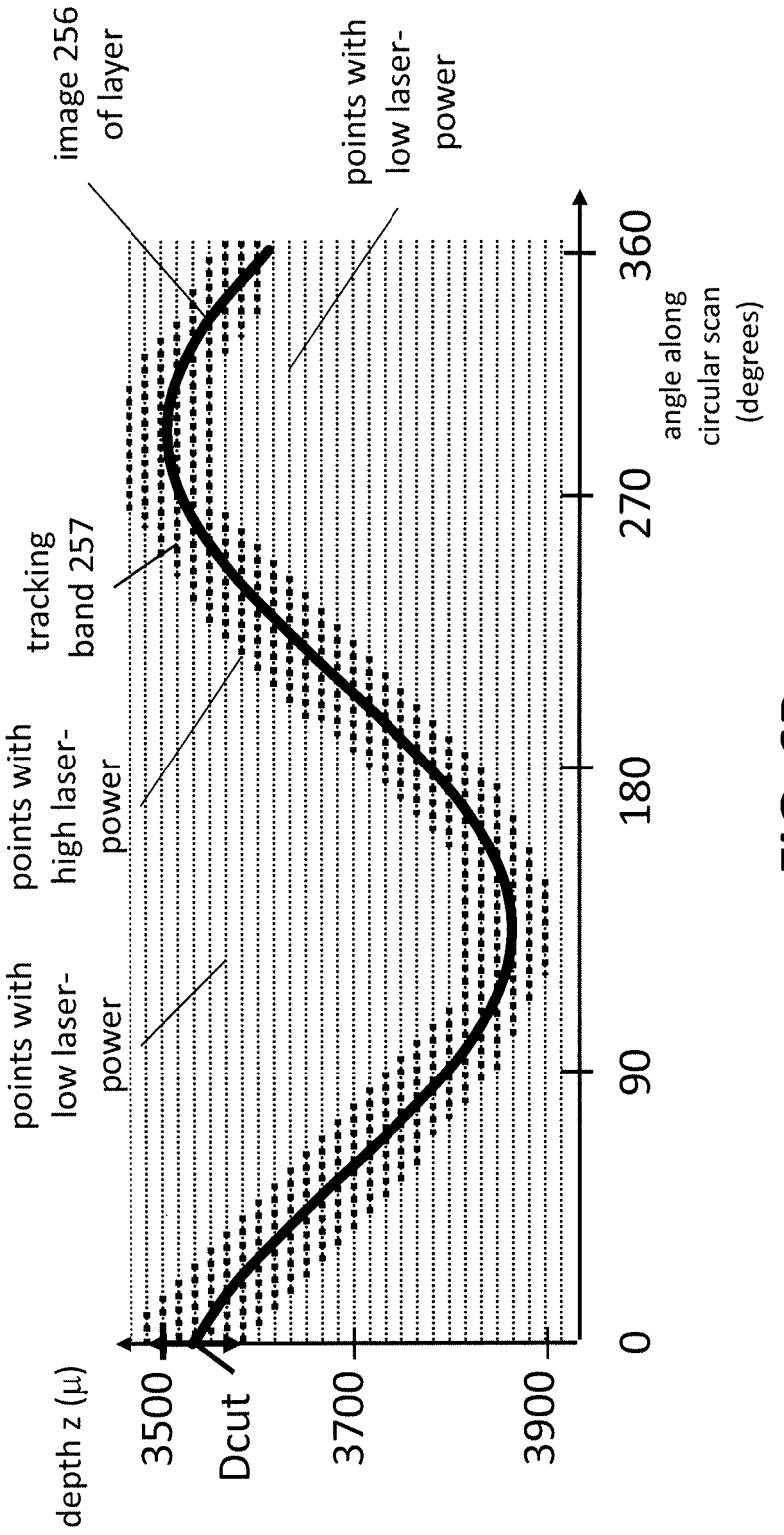
image 256 of layer
points with low laser-power
tracking band 257
points with high laser-power
points with low laser-power
depth z (μ)
3500
Dcut
3700
3900
0
90
180
270
360
angle along circular scan (degrees)

FIG. 6B

FIG. 6C

FIG. 6D

FIG. 6E

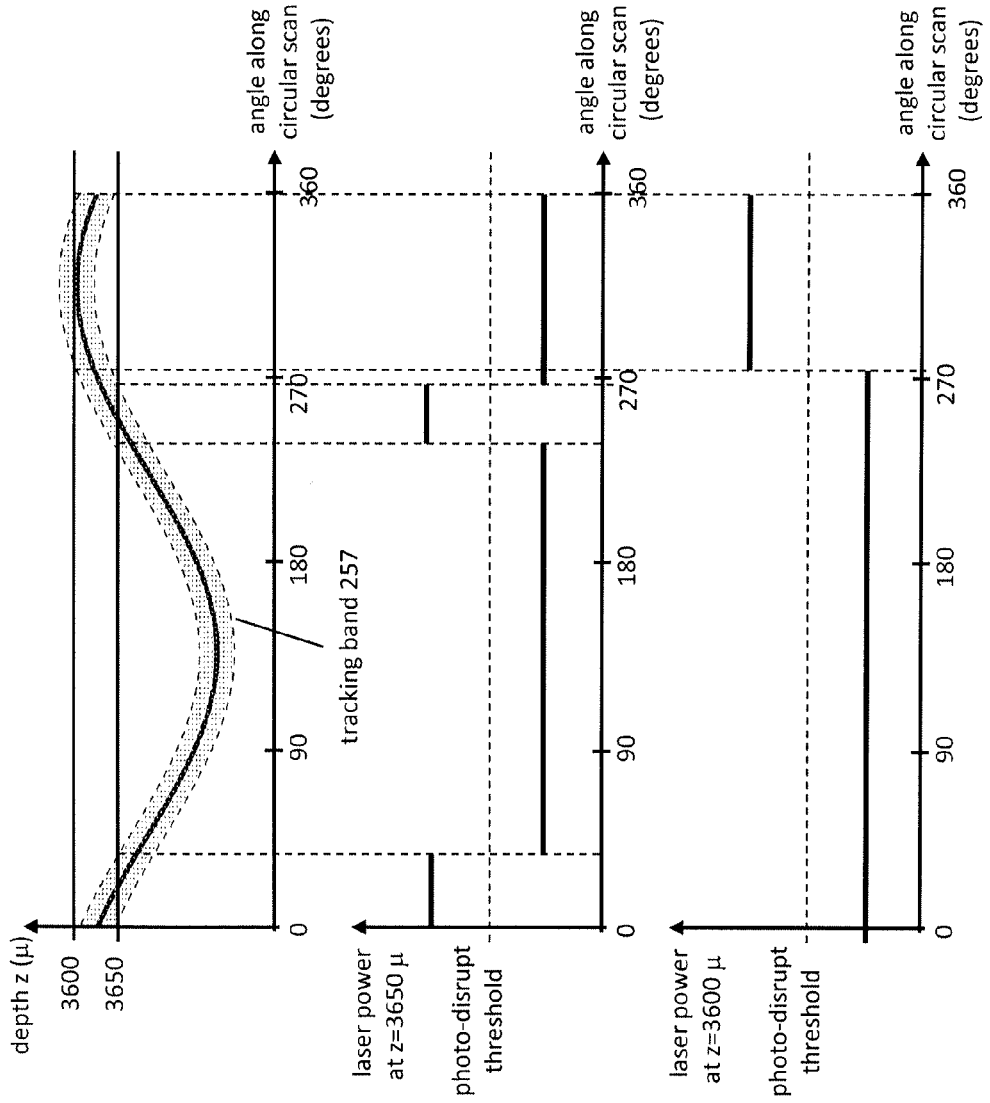

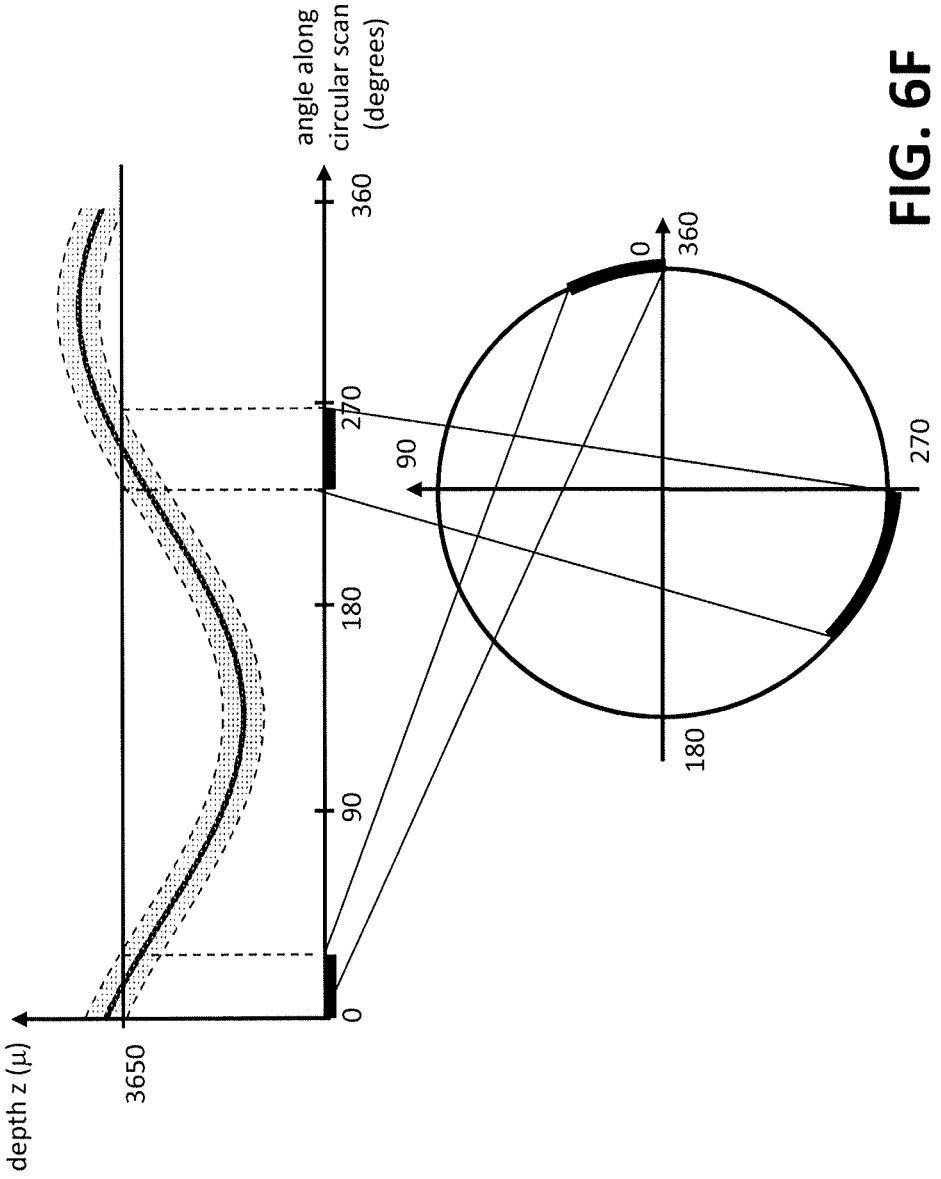
angle along circular scan (degrees)
360
270
180
90
0
depth z (μ)
3650
0
360
90
270
180

FIG. 6F

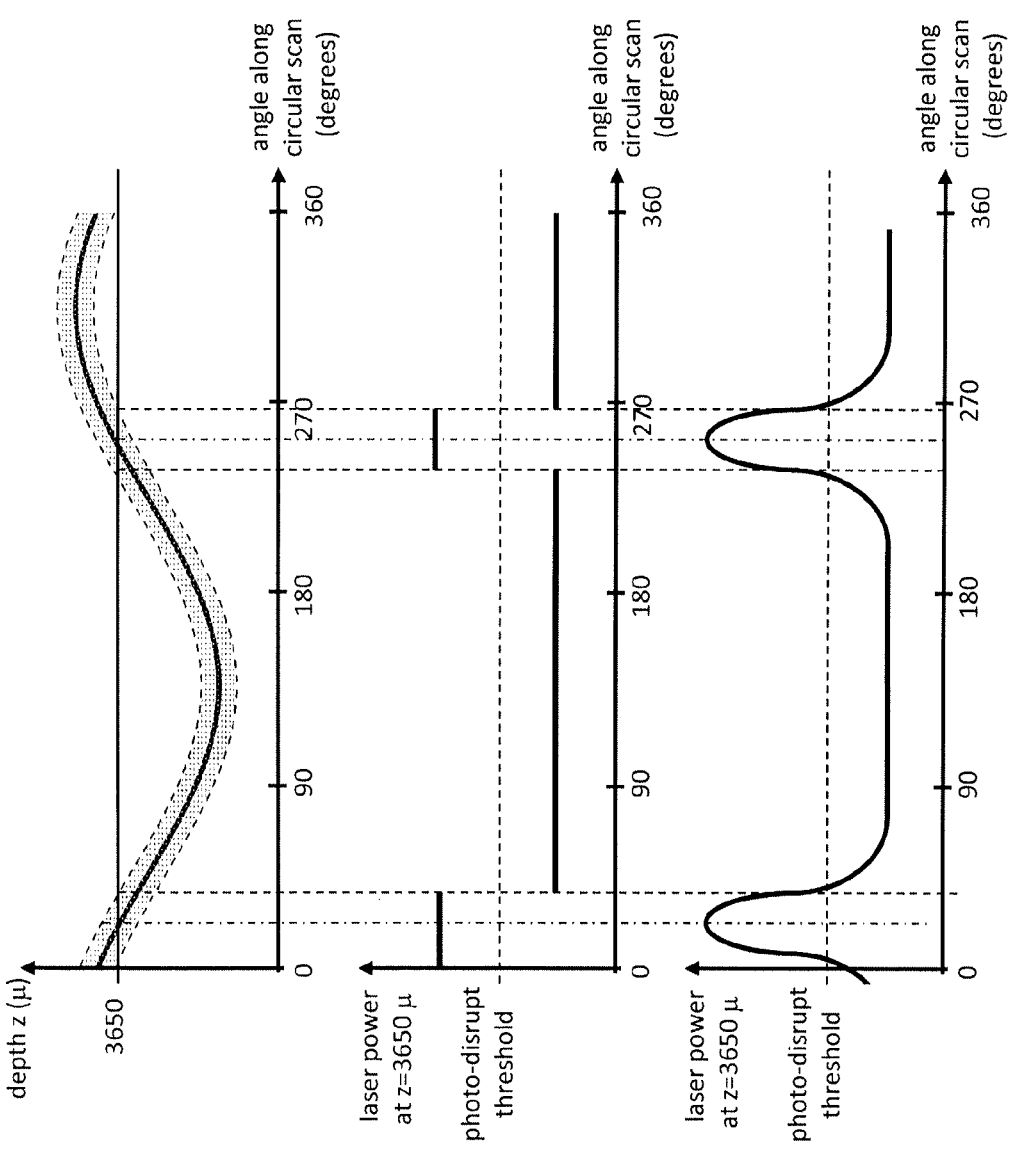
depth z (μ)
3650
angle along circular scan (degrees)
0
90
180
270
360
laser power at z=3650 μ
photo-disrupt threshold
angle along circular scan (degrees)
0
90
180
270
360
laser power at z=3650 μ
photo-disrupt threshold
angle along circular scan (degrees)
0
90
180
270
360

FIG. 6G

FIG. 6H

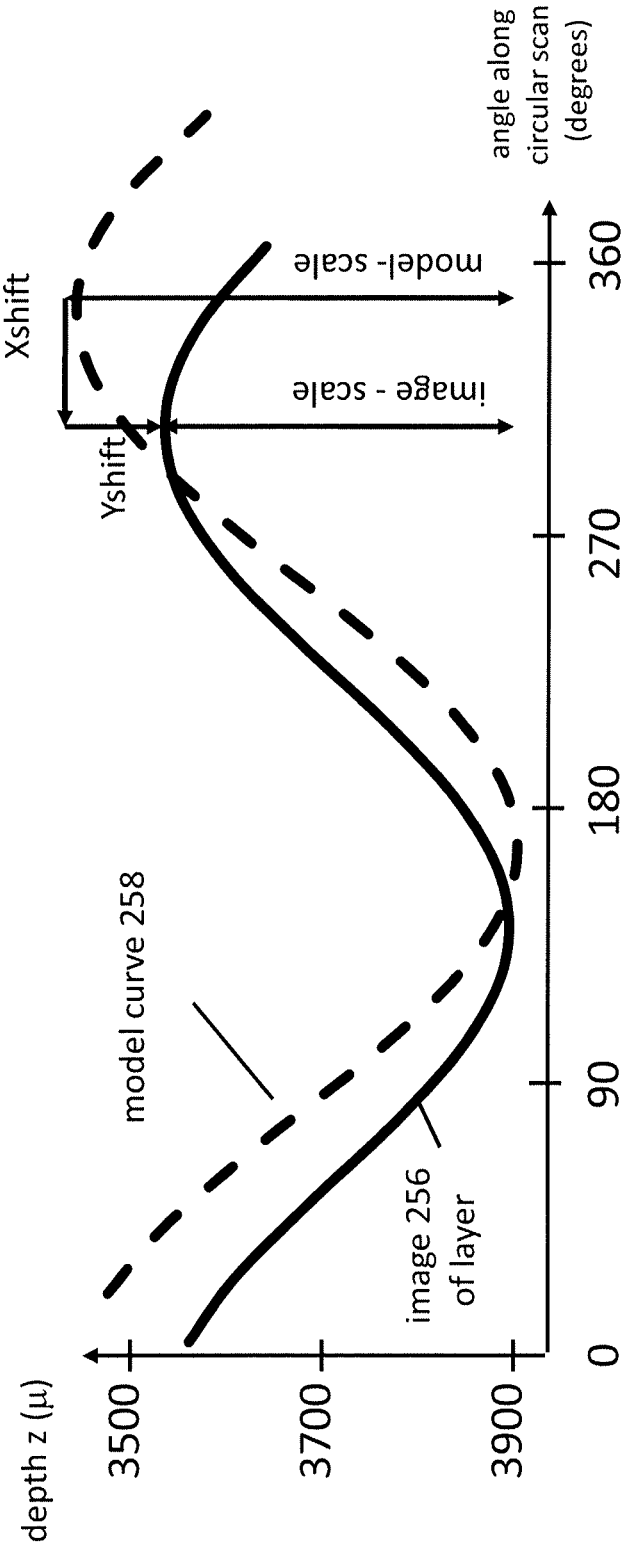
depth z (μ)
3500
3700
3900
0
90
180
270
360
angle along circular scan (degrees)
model curve 258
image 256 of layer
Xshift
Yshift
model- scale
image - scale

FIG. 7

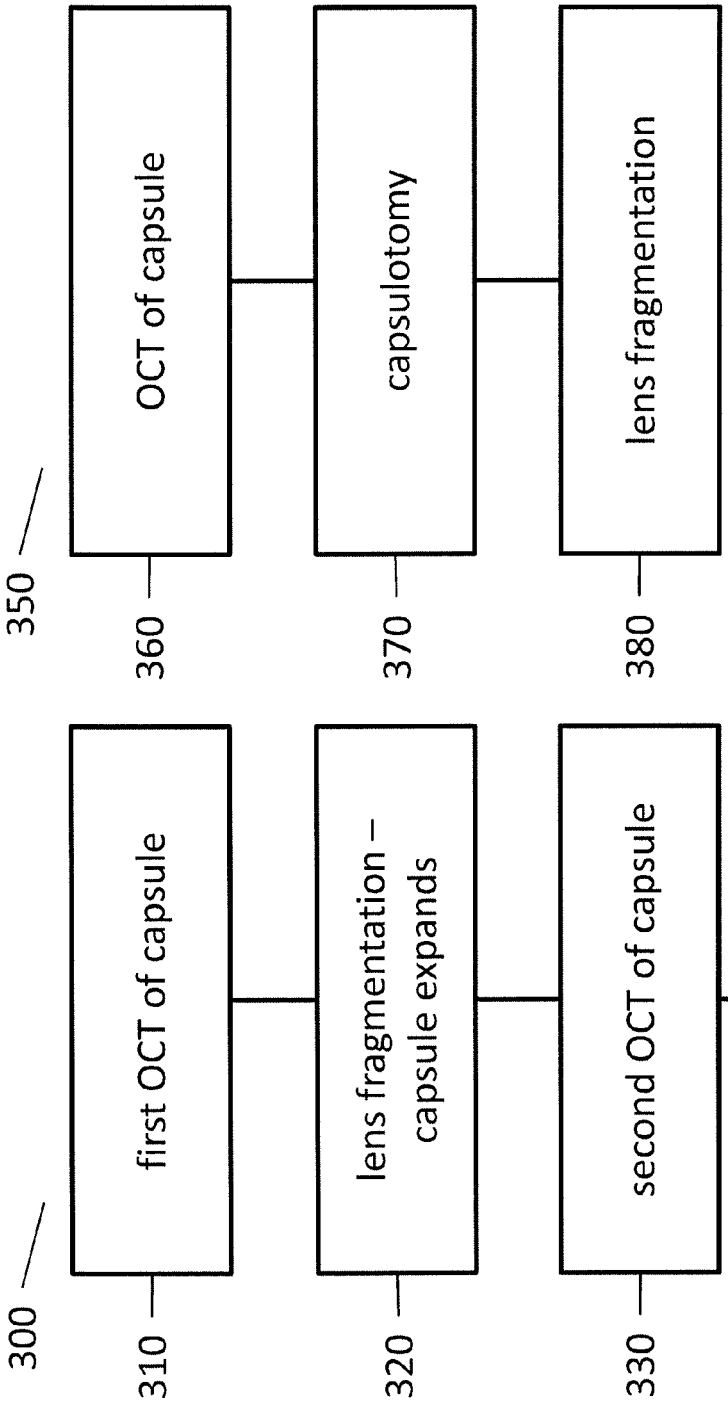
300
310
first OCT of capsule
320
lens fragmentation – capsule expands
330
second OCT of capsule
340
capsulotomy
350
360
OCT of capsule
370
capsulotomy
380
lens fragmentation

FIG. 8A

FIG. 8B

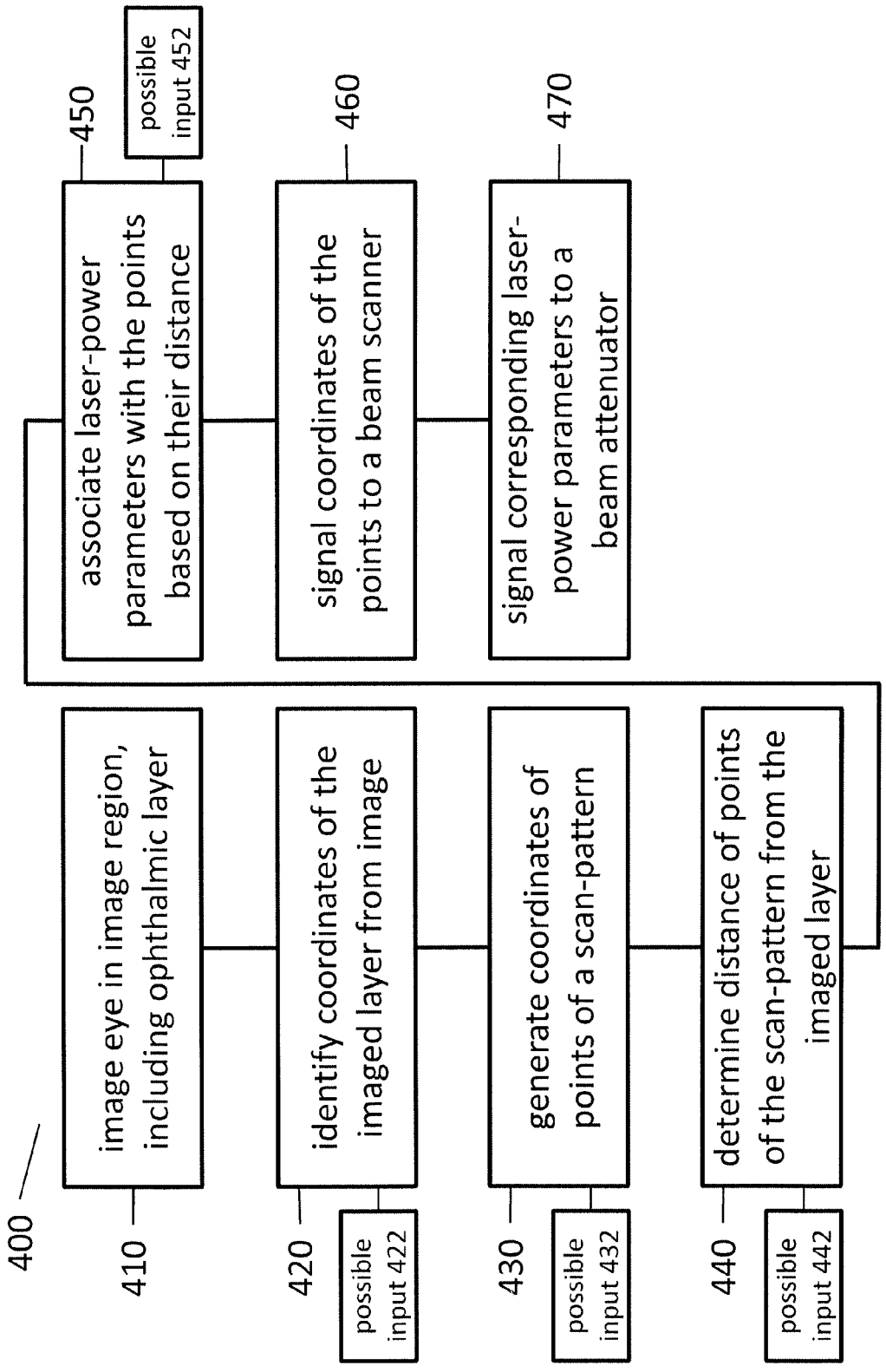
400
410
image eye in image region, including ophthalmic layer
420
identify coordinates of the imaged layer from image
possible input 422
430
generate coordinates of points of a scan-pattern
possible input 432
440
determine distance of points of the scan-pattern from the imaged layer
possible input 442
450
associate laser-power parameters with the points based on their distance
possible input 452
460
signal coordinates of the points to a beam scanner
470
signal corresponding laser-power parameters to a beam attenuator

FIG. 9

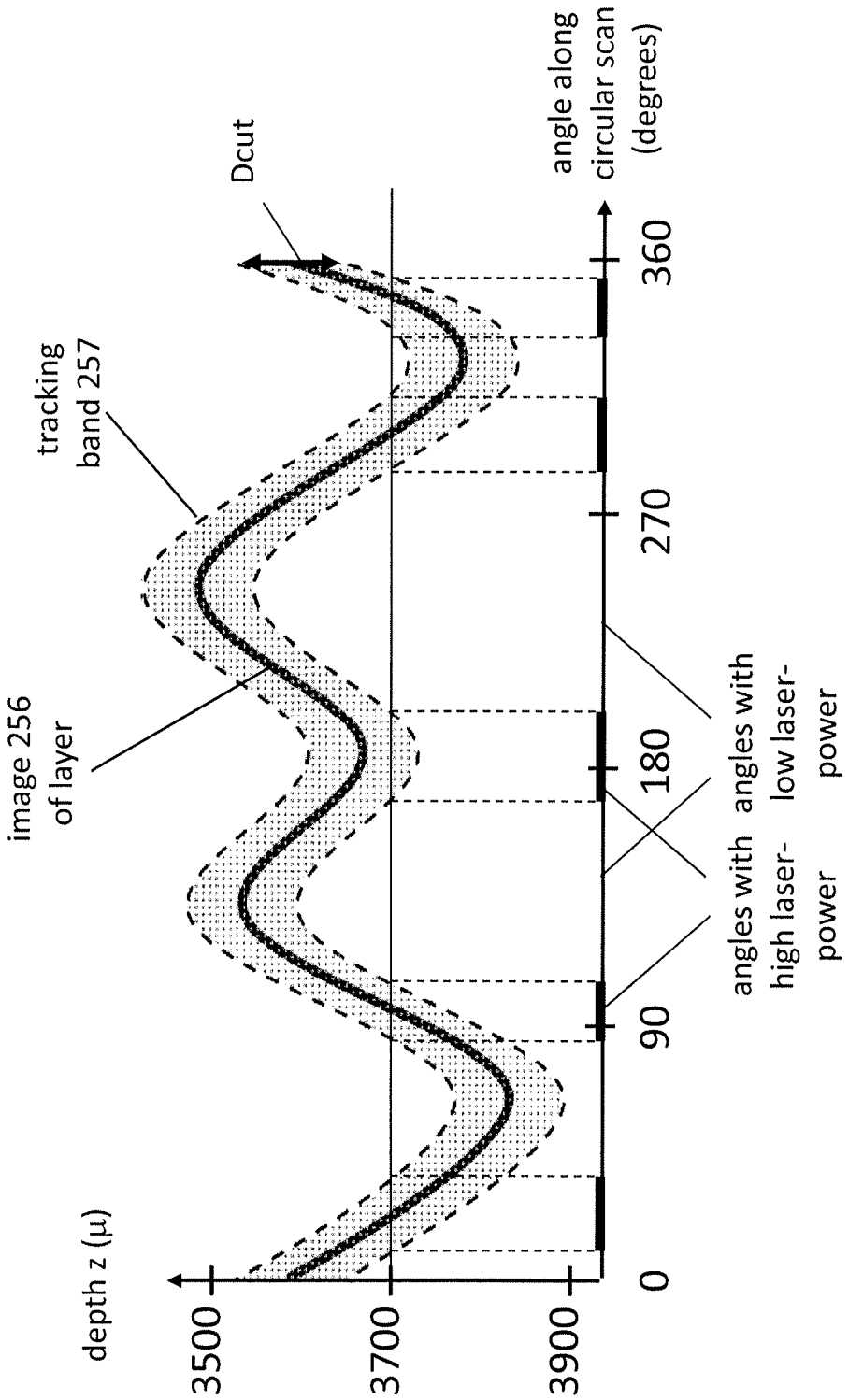
depth z (μ)
3500
3700
3900
0
90
180
270
360
angle along circular scan (degrees)
Dcut
tracking band 257
image 256 of layer
angles with high laser-power
angles with low laser-power

FIG. 10

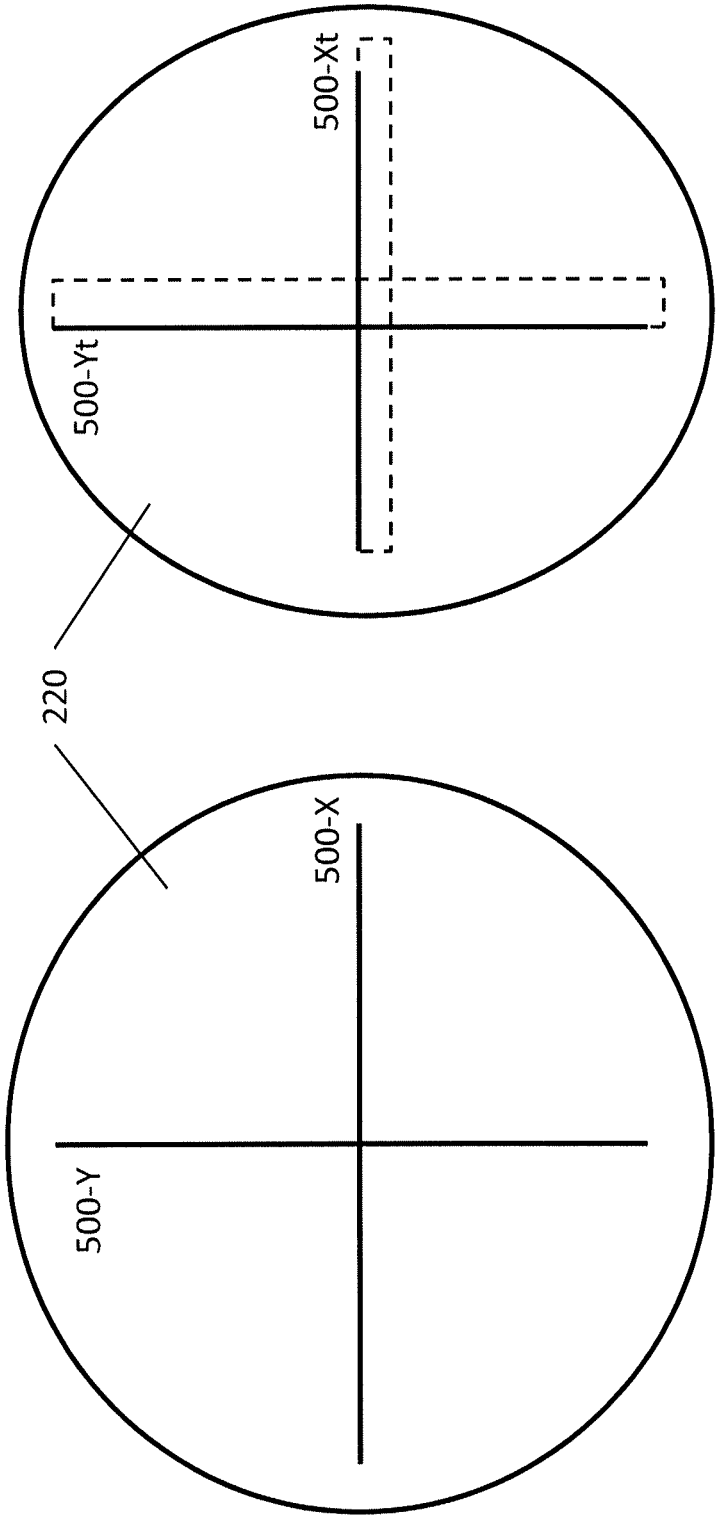

FIG. 11B

FIG. 11A

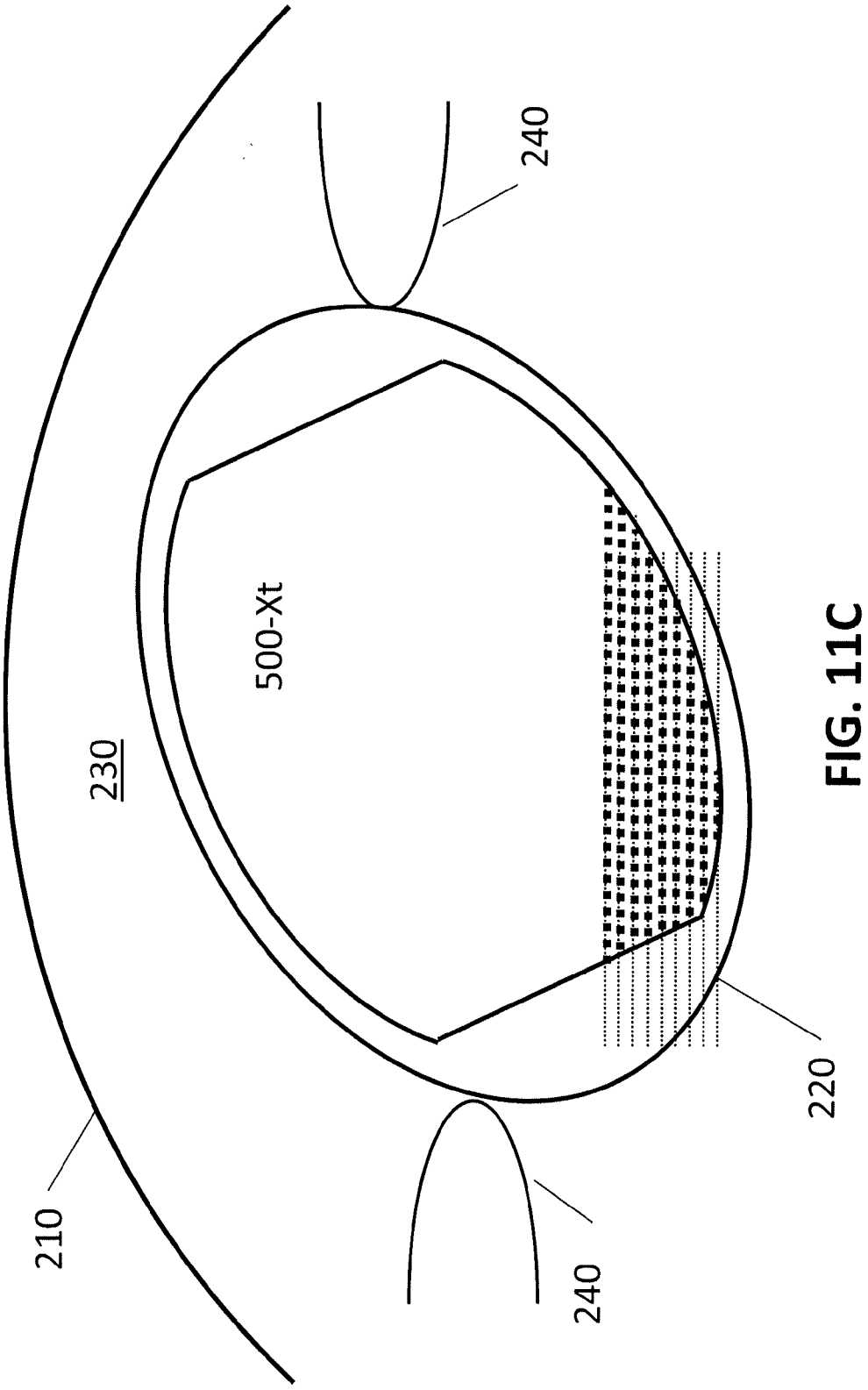

FIG. 11C

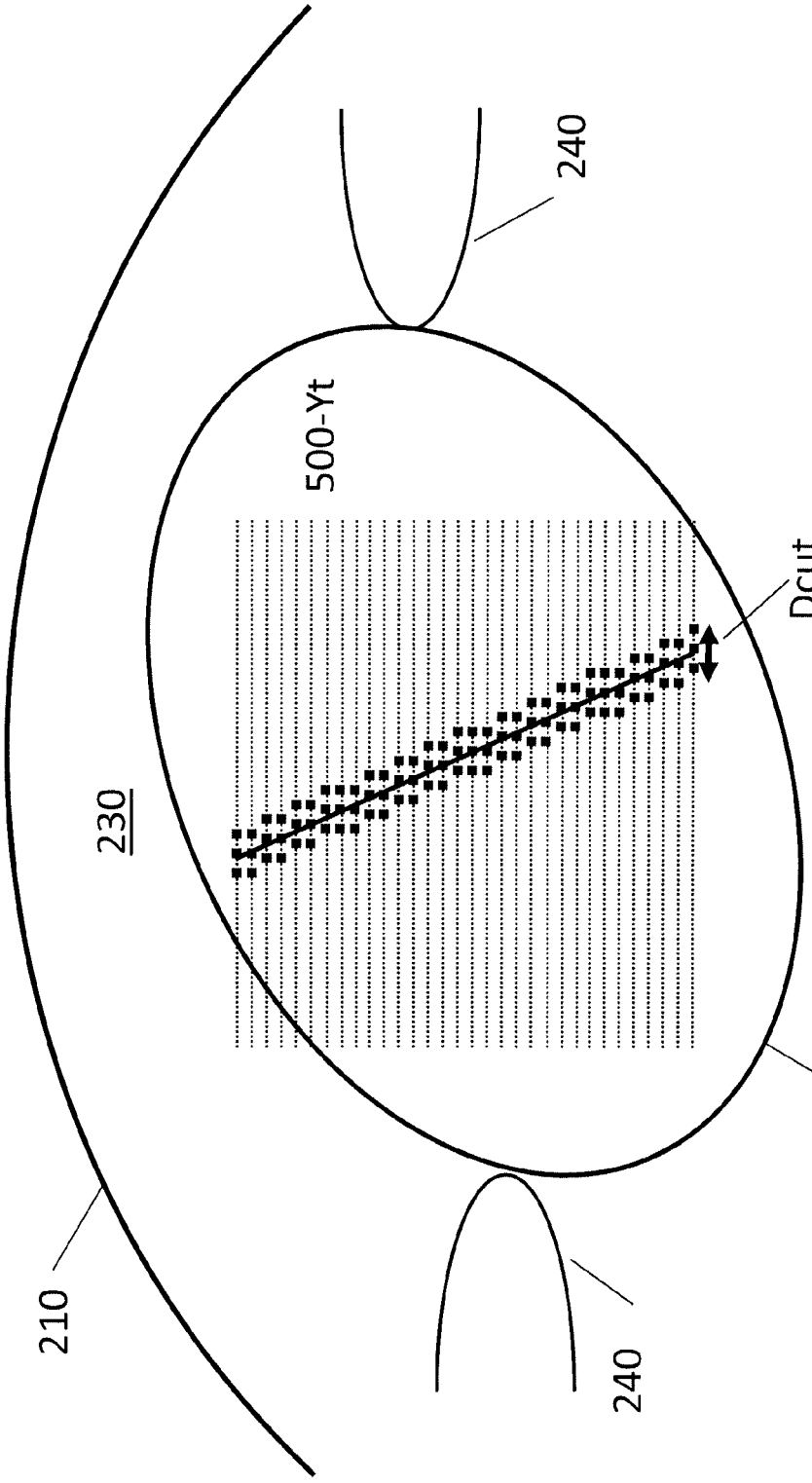

FIG. 11D

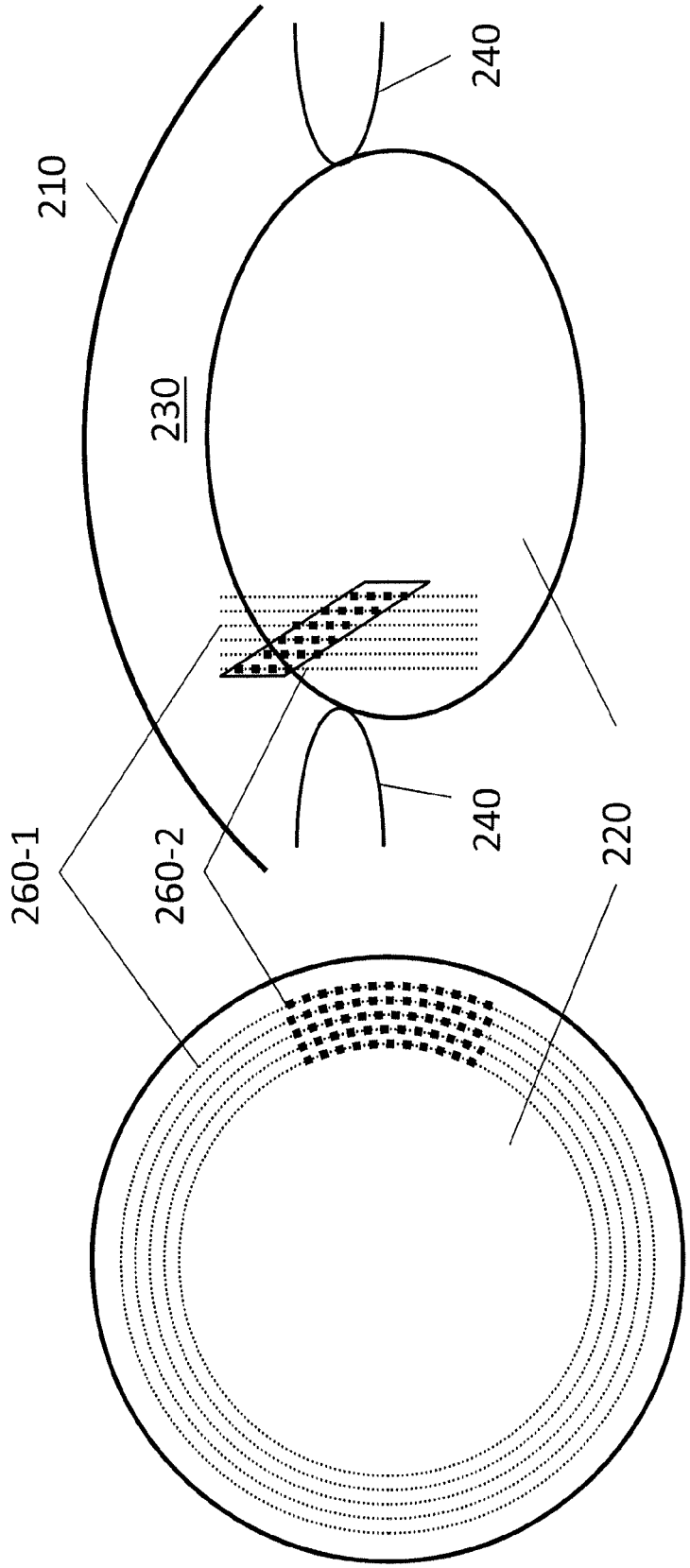

FIG. 12A

FIG. 12B

IMAGING-CONTROLLED LASER SURGICAL SYSTEM

TECHNICAL FIELD

This patent document describes a system and method for controlling a laser in an ophthalmic procedure. In more detail, this patent document describes an imaging-controlled laser system for controlling the power of a pulsed ophthalmic laser during capsulotomy and cataract procedures, among others.

BACKGROUND

Laser systems have become essential for ophthalmic surgery. They have been employed in corneal procedures for some time now with high precision and therefore considerable success. In very recent times applications for other ophthalmic procedures have been contemplated, including cataract procedures.

Lasers can be used for forming high precision cuts. These cuts are created by focusing or directing a rapid sequence of laser pulses to a scan-pattern or point-pattern. The points of the scan-pattern often form a line or layer and the laser pulses are directed to these points by a scanning system that includes deflection devices, mirrors and lenses whose alignment can be changed very quickly. In typical laser systems the pulses can have a duration or pulse length in the nanosecond, picosecond, or even femtosecond range. The pulse repetition rate can be in the kHz to hundreds of kHz range.

The power or energy of the laser pulses can be chosen to exceed a so-called photodisruption threshold. Laser pulses with a power above this threshold can disrupt the ophthalmic tissue at the target points, inducing the formation of bubbles. Lines or layers of these bubbles can weaken the mechanical connection between the tissue-portions on the opposite sides of the bubbles. Often the weakening is substantial, effectively cutting the tissue. Therefore, a subsequent manual procedure can completely separate the tissue portions with ease.

One ophthalmic procedure which could benefit from using such a high precision laser cutting system is cataract surgery. A typical cataract surgery involves a capsulotomy step and a lysis or lens fragmentation step. During lysis, energy is applied to a lens nucleus to liquefy it. During lens fragmentation, or phaco-fragmentation, the nucleus of the lens can be cut into several pieces by scanning the laser along cutting surfaces to enable the subsequent piece-by-piece removal of the nucleus. The capsulotomy involves forming a circular cut on the anterior portion of the capsular bag of the lens to allow the surgeon to access and remove the cut-up pieces of the nucleus.

To optimize surgical laser systems for these complex ophthalmic procedures is a great challenge. However, the optimization promises great returns in terms of the precision and efficacy of the surgical procedures.

SUMMARY

One of the challenges of laser cataract surgery is that the procedures of capsulotomy and lens fragmentation can interfere with each other. In advanced laser systems the precision of the surgery can be enhanced by imaging the ophthalmic target tissue prior to the surgery and guide the laser pulses based on the image. If the lens fragmentation is performed first, then, as a surgical by-product, the capsule is expanded considerably and unevenly by the substantial amount of bubbles formed inside the capsule. Therefore, after the lens fragmentation, the capsule and lens has to be imaged for a second time to guide the subsequent circular cut of the capsulotomy. However, imaging the severely photodisrupted and distorted lens can be challenging. Also, the repeated imaging procedure consumes precious surgical time, increasing the discomfort of the patient, potentially undermining the precision of the entire procedure.

On the other hand, if the capsulotomy is performed first, it creates a substantial amount of bubbles in the anterior region of the lens and in the anterior aqueous chamber of the eye. The amount of bubbles is especially high if the lens is in a tilted position before the procedure, as explained below. These bubbles can increase the scattering of the laser pulses of the subsequent lens fragmentation considerably as the subsequent pulses are directed to the inside of the lens and thus propagate through the bubble-rich anterior region. The increased scattering can again potentially undermine the precision of the cataract procedure.

Thus, both sequences of the lens fragmentation and capsulotomy have drawbacks, as the first step can reduce the precision and control of the subsequent step. Therefore, laser systems that reduce, resolve, or eliminate one or more of these drawbacks can offer advantages.

Embodiments of the present invention can provide advantageous functionalities in view of these challenges. In particular, an embodiment of an imaging-based laser system can include a laser-beam system, configured to generate and scan a beam of laser pulses with an adjustable laser-power parameter to points of a scan-pattern in an eye, and an imaging-based laser-controller, configured to image a layer in the eye, to control the scanning of the beam of laser pulses to the points of the scan-pattern, and to control a laser-power parameter of the laser pulses according to the distance of the points of the scan-pattern from the imaged layer.

An implementation of an imaging-based laser system can include a laser that generates and directs a beam of laser pulses into an eye, an imaging system that images a capsule layer of the eye, and a laser control system that controls the laser to direct the beam to spots within a tracking band of the imaged capsule layer with a laser-power parameter above a photo-disruption threshold, and to spots outside the tracking band of the imaged capsule layer with a laser-power parameter below a photo-disruption threshold, wherein the image-based laser system is configured to perform a capsulotomy before a lysis or lens- or phaco-fragmentation during a cataract procedure.

An implementation of an image-guided ophthalmic laser system can include a laser engine, configured to generate laser pulses, a beam modifier, configured to modify a laser-power parameter of the laser pulses, a laser scanner, configured to direct the laser pulses to scanning-points in an eye, an imaging system, configured to image a region in the eye, and a pattern generator, coupled to the imaging system, the beam modifier and the laser scanner, configured to generate coordinates of the scanning-points for the laser scanner, and to associate a laser-power parameter with the scanning-points depending on a distance of the scanning-points from a target-pattern.

In some implementations, a method of performing an imaging-controlled ophthalmic procedure can include imaging a layer in an eye, generating coordinates of points of a scan-pattern, determining a distance of the points of the scan-pattern from the imaged layer, and associating laser-power parameters with the points based on the determined distance.

BRIEF DESCRIPTION OF THE DRAWINGS

FIG. **1** illustrates an embodiment of a surgical laser system with an imaging-controlled laser system

FIGS. **2**A-D illustrate embodiments of the laser-beam system.

FIGS. **3**A-E illustrate embodiments of the imaging-based laser controller.

FIGS. **4**A-B illustrate the scan-patterns for non-tilted and tilted lenses.

FIGS. **5**A-B illustrate traditional scan-patterns for non-tilted and tilted lenses as a function of a scanning variable.

FIGS. **6**A-H illustrate a scan-pattern along a circular scan with a distance-dependent laser-power parameter.

FIG. **7** illustrates a determination of the z-depth of the imaged layer by using a model curve.

FIG. **8**A-B illustrate methods of cataract surgery with the lens fragmentation and capsulotomy in different sequences.

FIG. **9** illustrates a method of cataract surgery with an imaging-controlled laser system in detail.

FIG. **10** illustrates a multi-extrema tracking-band laser scan-pattern after lens-fragmentation expanded the lens capsule in a non-uniform manner.

FIGS. **11**A-D illustrate scan-patterns for tilted chop cuts.

FIGS. **12**A-B illustrate scan-patterns for tilted volume cuts.

DETAILED DESCRIPTION

Implementations and embodiments described in this patent document offer improvements for the above described challenges.

FIG. **1** illustrates an imaging-based laser system **100**, including a laser-beam system **110** to generate and scan a beam of laser pulses with an adjustable laser-power parameter to points of a scan-pattern in an eye **1**, and an imaging-based laser-controller **120** to image a layer in the eye, to control the scanning of the beam of laser pulses to the points of the scan-pattern, and to control a laser-power parameter of the laser pulses according to the distance of the points of the scan-pattern from the imaged layer. The laser-controller **120** can perform these functions by sending a power control signal and a scanning control signal to the laser-beam system **110**, for example.

The laser beam of the laser-beam system **110** can be guided into the main optical pathway at a beam-splitter **132-1** that can redirect the beam to an objective **134**. The beam can propagate through the objective **134** and through a patient interface **136** to enter into the surgical eye **1**.

The surgery can be assisted by imaging the eye **1** with various techniques. A visible imaging light can be used to create a video image that is processed by a video microscope **138**. In addition, the imaging-based laser-controller **120** can shine an imaging beam on the eye and form an image based on the returned image beam. This imaging beam can be coupled into and out of the main optical path by a beam-splitter **132-2**.

FIGS. **2**A-D illustrate various embodiments of the laser-beam system **110**.

FIG. **2**A illustrates that embodiments of the laser-beam system **110** can include a laser engine **112** to generate the beam of laser pulses, a beam attenuator **114** to modify the laser-power parameter of the laser pulses, and a beam scanner **116** to direct the beam of laser pulses to the points of the scan-pattern in the eye. The laser engine **112** can generate laser pulses with a duration of nanoseconds, picoseconds or even femtoseconds, i.e. in the 10^{-9}-10^{-15} sec range. These pulses can be generated at a repetition rate in a wide range of frequencies: from 0.1 kHz to 1,000 kHz, or in a range of 1 kHz to 500 kHz, or in some implementations in the 10 kHz to 100 kHz range. The power control signal of the laser-controller **120** can be coupled into the beam attenuator **114** and the scanning control signal of the laser-controller **120** can be coupled into the beam scanner **116**.

The beam attenuator **114** can include a Pockels cell, a polarizer-assembly, a mechanical shutter, an electro-mechanical shutter, or an energy wheel. Each of these implementations can modify a laser-power parameter of the laser pulses. The laser-power parameter can be a pulse energy, a pulse power, a pulse length or a pulse repetition rate of the laser pulses, among others. The beam attenuator **114** can modify one or more of these laser-power parameters. In a simple implementation, the beam attenuator **114** can shutter or block selected laser pulses. In another, a polarizer assembly can reduce the power of selected laser pulses by adjusting the relative angle of subsequent polarizing filters.

In the embodiment of FIG. **2**A, the beam attenuator **114** can be located between the laser engine **112** and the beam scanner **116** in the path of the laser beam.

FIG. **2**B illustrates and embodiment in which the beam attenuator **114** is at least partially integrated into the laser engine **112**. In some cases, the beam attenuator **114** can be part of the laser engine **112**. For example, a Pockels cell within the laser engine **112** can be the beam attenuator **114**.

FIG. **2**C illustrates and embodiment in which the beam attenuator **114** is located after the beam scanner **116** in the path of the laser beam.

Finally, FIG. **2**D illustrates an embodiment in which the beam attenuator **114** and the beam scanner **116** are at least partially integrated.

FIGS. **3**A-E illustrate various embodiments of the imaging-based laser-controller **120**.

FIG. **3**A illustrates that the laser-controller **120** can include an imaging system **122** to image the imaged layer in the eye and a pattern generator **124** to generate coordinates of the points of the scan-pattern, to associate laser-power parameters with the points depending on the distance of the points from the imaged layer, and to signal the generated coordinates of the points and the corresponding laser-power parameters to the laser-beam system **110**. In some implementations, the imaging system **122** can image any ophthalmic target in the anterior or posterior segment of the eye, targets from the cornea to the retina.

The pattern generator **124** can signal the generated coordinates of the points of the scan-pattern to the beam scanner **116** with a scanning control signal. Further, the pattern generator **124** can signal the laser-power parameters corresponding to the points of the scan-pattern to the beam attenuator **114** with a power control signal. The laser-power parameter can be a pulse energy, a pulse power, a pulse length or a pulse repetition rate of the laser pulses.

The imaging system **122** can include an ophthalmic coherence tomography (OCT) system, a Scheimpflug imaging system, a scanning imaging system, a single shot imaging system, an ultrasound imaging system, and a video imaging system. Here, the scanning imaging systems can create the image by scanning an imaging beam, whereas single shot imaging systems can acquire imaging information about an imaged area or volume in a single shot. The OCT system can be a time-domain OCT, a frequency-domain OCT, or a spectrometer-based OCT system, among others.

FIG. **3**B illustrates that in some implementations the laser-controller **120** can include an image-analyzer **126**. The

image analyzer **126** can receive the image of the imaged layer from the imaging system **122**, perform an analysis of the imaged layer as described below and forward the result of the analysis to the pattern generator **124**.

FIG. **3**C illustrates that in some implementations the image analyzer **126** can be at least partially integrated with the imaging system **122**. FIG. **3**D illustrates that in some implementations the image analyzer **126** can be at least partially integrated with the pattern generator **124**.

FIG. **3**E illustrates that in some embodiments, the laser system **100** can include an operator-interface **128** that can be coupled to one or more of the imaging system **122**, the pattern generator **124** and the image analyzer **126**.

FIGS. **4**A-B set the stage to illustrate the operation of the laser system **100**. The imaging system **122** can image the imaged layer in an image region that can be based on a loop, an arc, a line, or a two-dimensional pattern transverse to a z-axis of the imaging system, and extends to a depth range Dimage along the z-axis of the imaging system. The imaging system **122** can support a determination of a z-depth coordinate of the imaged layer corresponding to a scanning coordinate along an image-scan.

FIG. **4**A illustrates that the imaging system **122** can perform an imaging relevant for a capsulotomy step of a cataract procedure. The schematic cross section illustrates the anterior segment of the eye **1**. The outermost layer is a cornea **210**. A crystalline lens **220** is located behind the cornea **210**, separated from it by an aqueous anterior chamber **230**. The crystalline lens **220** is encapsulated in a thin capsule or capsular bag **222**. The lens **220** is held in place by ciliary muscles **240**. These muscles **240** also adjust the shape of the crystalline lens **220** as needed for bringing objects into focus.

As it has been described above, in order to facilitate the removal of a fragmented nucleus of the lens **220**, the cataract surgery typically involves creating a circular capsulotomy cut **250** on the capsular bag **222**. As a first step, the imaging system **122** can create an image **252** of the anterior segment of the eye by scanning along a scanning circle **254** and imaging the eye in a depth-range Dimage, defining an image-cylinder **260**-*i*.

FIG. **5**A illustrates that the image **252** typically includes an image **256** of the imaged anterior capsule layer of the lens **220** "unfolded" along a scanning variable, such as an angle along the circumference of the scanning circle **254**. If a z-axis of the lens **220** is aligned with a z-axis of the laser system **100**, the image **256** of the imaged layer is a flat line, indicating an essentially constant z-depth.

In other implementations, the image **252** can include the image of other ophthalmic targets, including corneal layers, portions of the sclera and even retinal layers. The zero depth level can be defined in a large number of ways, using a lens of the objective **134**, a reference mirror of the imaging system **122**, a level of the patient interface **136**, or a level of an ophthalmic structure, such as the cornea **210**.

By analyzing the image **252**, a surgeon can recognize the image **256** of the imaged layer. Based on the z-depth of the imaged layer, the surgeon can decide where to direct the cutting laser beam to form the capsulotomy cut **250**. The cutting laser beam is typically scanned along the same scanning circle **254** to form a cut-cylinder **260**-*c* with a depth-range Dcut, typically smaller than Dimage. This way the placement of the cut-cylinder **260**-*c* benefits maximally from the information contained in the image **252**, and in particular in the image **256** of the imaged layer. The capsulotomy cut **250** is formed where the cut-cylinder **260**-*c* intersects the lens capsule **222**. In practice, the cut cylinder **260**-*c* is often formed as a stack of bubble-circles, where the individual circles are created by directing the laser pulses along a circular scan-pattern at a fixed z-depth to cause photodisruption, followed by the formation of a similar circle at a slightly lesser z-depth.

In some typical cases, the image depth-range Dimage can be 5-10 millimeters, whereas the cut depth-range Dcut can be in the range of 50-200 microns, in some cases 75-150 microns, sometimes approximately 100 microns.

It is noted that the bubbles of the cut-cylinder **260**-*c* can scatter and deflect laser pulses applied in subsequent surgical steps. For example, in a cataract surgery the capsulotomy can be followed by the lens fragmentation or lysis. The bubbles of the cut-cylinder **260**-*c* can negatively impact the precision and efficiency of this subsequent lens-fragmentation by scattering the lens-fragmenting laser pulses.

Fortunately, when a z-axis of the lens **220** is parallel to a z-axis of the laser system **100**, the depth range Dcut of the cut cylinder **260**-*c* can be as little as 100 microns, creating only a limited number of bubbles. Thus, in the case of a well-aligned lens **220**, the bubbles of the cut-cylinder **260**-*c* introduce only a limited amount of scatter for the subsequent lens fragmentation laser pulses.

FIG. **4**B illustrates, however, that in the typical surgical case the crystalline lens **220** can be tilted. This situation can occur for a variety of reasons. For example, the weight of the objective **134** can push the lens **220** sideways upon docking to the eye **1**. Or, applying suction at the patient interface **136** to immobilize the eye **1** can lead to a tilting of the lens **220** as well.

FIG. **5**B illustrates the image **252** of such a tilted lens **220** unfolded along the angular scanning variable of the scanning circle **254**. In contrast to the non-tilted case of FIG. **5**A, the image **256** of the tilted imaged layer can exhibit substantial sinusoidal oscillations. The amplitude of these oscillations can be as much as 300-500 microns. To make sure that the capsular bag **222** is cut everywhere along this sinusoid, the cut-cylinder **260**-*c* can be formed with a much enlarged depth-range Dcut, exceeding the amplitude of the sinusoid. In the above example, Dcut can be 400-600 microns to be sure that the capsular bag **222** was cut along the entire sinusoid. Clearly, this approach may create 4-6 times more photodisrupted bubbles during capsulotomy than the procedure for a non-tilted lens. Capsulotomy bubbles in such an increased number can scatter the laser pulses of the subsequent lens fragmentation to a substantial degree, threatening its precision and efficacy.

FIGS. **6**A-H illustrate that some implementations of the laser system **100** can substantially reduce the number of photodisrupted bubbles by generating bubbles only in a narrow proximity of the imaged layer.

As described above, this outcome can be achieved, for example, by the imaging-based laser-controller **120** imaging the capsular bag **222**, controlling the scanning of the beam of laser pulses to the points of the scan-pattern, and controlling a laser-power parameter of the laser pulses according to the distance of the points of the scan-pattern from the imaged layer.

FIGS. **6**A-B illustrate that as the laser pulses are directed to points of the scan-pattern, the laser controller **120** can modify or adjust a laser-power parameter of the pulses. In particular, when a laser pulse is directed to a point of the scan pattern that is within a Dcut distance from the image **256** of the imaged layer along the z axis, the laser-controller **120** can adjust its laser-power parameter to a high value, e.g. above a photodisruption threshold. Whereas, when a laser pulse is directed to a point of the scan pattern that is farther

than Dcut from the image **256** of the imaged layer, the laser-controller **120** can adjust its laser-power parameter value to a low value, such as below a photodisruption threshold.

The just-described method creates bubbles only in a Dcut proximity of the imaged layer and therefore substantially reduces the number of bubbles to a value close to the number of bubbles for a well-aligned lens. For this reason, the scattering of the subsequent lens-fragmenting laser pulses by these capsulotomy bubbles is substantially reduced. Using the earlier value of Dcut being 400-600 microns for a tilted lens and 100 microns for a non-tilted lens, the present method may reduce the scattering of the lens-fragmenting bubbles by a factor of 4-6: a considerable gain in precision and control.

FIG. **6**A illustrates the implementation when the scanning of the capsulotomy laser pulses of the scan-pattern is performed along the z-axis for fixed points of the circular scan. FIG. **6**B illustrates the implementation when the scanning is performed along the circular scan with a fixed z-depth. This implementation can be used to create the above mentioned stacked circles. In either implementation, the points with high laser-power are placed within a tracking band **257** with a z-extent of Dcut.

FIGS. **6**C-E illustrate the implementation when the laser pulses are scanned at fixed z-depths along the circular scan. A tracking band **257** can be defined as the set of points of the scan-pattern that are within the preselected distance Dcut from the image **256** of the imaged layer.

FIGS. **6**D-E illustrate the laser power parameter of the pulses along the circular scan at two selected z-depths of 3600 microns and 3650 microns in an unfolded representation. The laser-controller **120** can control the laser power of the pulses that are directed to points inside the tracking band **257** to be above a photo-disruption threshold, and the laser power of the pulses that are directed to points outside the tracking band **257** to be below the photo-disruption threshold. In this embodiment, photodisrupted bubbles are only generated at points within the tracking band **257**, achieving the above functionality of the laser system **100**.

FIG. **6**F expresses the same operation in a folded representation. Here the value of the laser power parameter is shown as a function of the angular scanning variable (typically the angle), projected on the scanning circle **254** itself. Again, for those points of the scan-pattern that lie within the tracking band **257**, the laser power is high—indicated by a thick line—whereas for those points that lie outside the tracking band **257**, the laser power is low.

FIGS. **6**G-H illustrate a related implementation, where the laser-power controller **120** controls the laser power parameter as a function of the distance of the points from the imaged layer, wherein the laser-power is a decreasing function of the distance. FIG. **6**G illustrates the implementation where this function is essentially a two-valued step-function. FIG. **6**H illustrates the implementation where this function is a continuous function, its value decaying with the increasing distance from the imaged layer. In some implementations, it may be easier to control the laser power in the continuous manner of FIG. **6**H.

The above-outlined implementations depend on the knowledge of the distance between the points of the scan-pattern and the imaged layer. Three stages are involved in determining this distance. First, the identity of the imaged layer is identified in the image **252** to determine the image **256** of the imaged layer. Then, the z-depth coordinate of the imaged layer is determined. Finally, the distance of the imaged layer and the points of the scan-pattern can be determined, for example, by taking the difference of the z-depth coordinates of the points of the scan-pattern and the imaged layer at the corresponding angular scanning coordinates, such as at the same angle.

Concerning the first step, the raw image **252** does not isolate or identify the imaged layer explicitly. Thus, establishing the identity of the imaged layer may necessitate an analysis of the image **252**. As discussed earlier, this analysis of the image can be performed by the imaging system **122**, the pattern generator **124**, or the image analyzer **126**, possibly assisted by an input from a system operator through the operator interface **128**.

FIG. **7** illustrates that the imaging system **122** can support the identification of the imaged layer and the determination of its z-depth coordinates in different ways. In some implementations the laser system **100** can include the operator interface **128** and the imaging system **122** can support the identification of the imaged layer using an input from an operator through the operator interface **128**.

For example, on a graphical user interface, or GUI, the operator interface **128** can prompt the operator to fit a model curve **258** to the spots in the image **252** representing the imaged layer. Since in the case of a tilted ellipsoid-shaped lens the image **256** of the imaged layer is typically a sinusoidal curve, the operator interface **128** can display a generic sinusoidal curve **258** on the GUI and prompt the operator to fit this model curve **258** to the layer-spots in the image **252**. Once the operator fitted the model curve **258** to the layer-spots in the image **252**, the model curve **258** can serve as the image **256** of the imaged layer.

The operator can achieve this task through various approaches: by shifting the model curve **258** by an Xshift in the X direction (i.e. adjusting the angle along the circular scan) and by shifting the model curve **258** by a Yshift in the Y direction (i.e. adjusting the z-depth coordinate). In other implementations the operator can be prompted to adjust the scale of the model curve **258** to the scale of the sinusoidally located layer-spots in the image **252**, i.e. to rescale the z-depth of the model curve **258** to fit the z-depth of the layer-spots. Many other fitting techniques can be implemented to achieve analogous functionalities.

The operator interface **128** can receive the input from the operator in many different ways, including through a keyboard, a touch-screen, a computer-communication channel, an external memory, a flash-drive, an internet connection, a speech-recognition apparatus or a wireless connection.

In other implementations, the determination of the identity and the z-depth of the imaged layer can be performed by the laser system **100** without the input of a surgeon or operator. In particular, the imaging system **122** can be configured to determine the identity and then the z-depth coordinate of the imaged layer by a processor or microcomputer performing a feature-recognition analysis of the image **252**. For example, the imaging system **122** can determine the identity and coordinates of the imaged layer by locating local maxima of the gradient of the spot intensity. In other implementations, an edge-recognition algorithm can be used. In these implementations, the imaging system **122** can identify the manifold of the maximum-gradient points as the image **256** of the imaged layer without resorting to fitting a model curve **258**. In some implementations, of course, the imaging system **122** can make use of a model curve **258** to identify the image **256** of the imaged layer.

In the above implementations, once the identity of the imaged layer has been determined in the image **252**, the z-depth coordinates of the imaged layer can be determined

in a straightforward manner, for example, by counting the pixels in the image **252**, or using a reference or a look-up table.

For the image analysis, the imaging system **122** can utilize a result of a pre-surgery measurement, statistical data, video image data, ophthalmic coherence tomography image data, or a model-based computation during the determination of the z-depth.

Once the z-depth of the imaged layer has been determined, the imaging system **122** can forward the z-depth and the corresponding scanning coordinates of the imaged layer to the pattern generator **124** to carry out the last stage, the determination of the distance between the imaged layer and the points of the scan-pattern, generated by the pattern generator **124**. This stage can be carried out, for example, by subtracting the z-depth coordinates of the points of the scan-pattern from the z-depth coordinates of the imaged layer that correspond to the same scanning variable, such as the same scanning angle.

Finally, having determined the distance of the points of the scan-pattern from the imaged layer, the pattern generator **124** can associate a laser-power parameter above a photodisruption threshold with those points that are closer to the imaged layer than a predetermined distance, and associate a laser-power parameter below a photodisruption threshold with those points that are farther from the imaged layer than the predetermined distance, as described in relation to FIGS. **6**A-H.

In some implementations, the imaging system **122** only captures the image **252** but does not identify the imaged layer or determine its z-depth coordinates. In these embodiments, the imaging system **122** can simply forward the unprocessed image **252** to the pattern generator **124** without analyzing it. The pattern generator **124** can receive the image **252**, identify the imaged layer and determine the z-depth coordinate of the imaged layer corresponding to a scanning coordinate along an image scan.

As above, in some implementations, the pattern generator **124** can determine the z-depth of the imaged layer by performing a feature-recognition analysis of the received image **252**. In other implementations, the pattern generator **124** can receive an operator input through the operator interface **128** during the process of determining the z-depth of the imaged layer, as described before.

In these implementations, once the z-depth coordinates of the imaged layer have been determined, the pattern generator **124** can define a tracking band **257** as a manifold of the points of the scan-pattern that are within a predefined distance from the coordinates of the imaged layer. Then the pattern generator **124** can associate a laser-power parameter above a photodisruption threshold with points of the scan-pattern inside the tracking band **257**, and a laser-power parameter below a photodisruption threshold with points of the scan-pattern outside the tracking band **257**.

Yet other implementations of the laser controller **120** may include an image analyzer **126** that can determine the z-depth coordinate of the imaged layer corresponding to a scanning coordinate along an image-scan. As was illustrated in FIGS. **3**B-D, the image analyzer **126** can be self-standing or at least partially integrated with the imaging system **122** or the pattern generator **124**.

The image analyzer **126** can identify the imaged layer and determine the z-depth coordinate of the imaged layer by performing a feature-recognition analysis of the image **252**. In other implementations, the image analyzer **126** can determine the z-depth coordinate by making use of an operator input through an operator-interface **128**.

The operation of the laser system **100** can be demonstrated on the example of the capsulotomy procedure, where the imaged layer is the lens capsule **222** between the lens **220** and the aqueous anterior chamber **230**. In this case, the scan-pattern corresponds to the cut-cylinder **260**-*c* intersecting the lens capsule **222** at the capsulotomy cut **250**. The pattern generator **124** can associate a photodisruptive laser-power parameter with points inside a tracking band **257** related to the intersection **250** of the cut-cylinder **260**-*c* and the lens capsule **222**, and a non-photodisruptive laser-power parameter with points outside the tracking band **257**.

FIG. **8**A illustrates a first cataract procedure **300** performed without the benefits of the laser system **100**. The cataract procedure **300** can be practiced when the capsulotomy generates an excessive number of bubbles as in FIGS. **4**B-**5**B. To prevent excessive scattering by these capsulotomy bubbles, the lens fragmentation is performed prior to the capsulotomy. In detail, the cataract procedure **300** can include a first imaging **310** of the capsule **222**, performed by an OCT procedure, followed by a lens fragmentation **320**. During the lens fragmentation **320** the capsule **222** expands because of the large number of bubbles generated in the crystalline lens **220**. The fragments of the lens **220** are removed through an opening, cut into the capsule **222** by a capsulotomy **340**. However, since the capsule **222** has expanded during the lens fragmentation **320**, the results of the first imaging **310** are not reliable anymore. Therefore, the capsulotomy **340** has to be preceded by a second imaging **330**. The second imaging **330** can take up precious surgical time and increase the discomfort of the patient. Both of these factors can endanger the efficacy of the cataract procedure **300**.

FIG. **8**B illustrates a cataract procedure **350** with an embodiment of the laser system **100**. Since the laser system **100** is capable of creating only a limited number of bubbles during the capsulotomy, the capsulotomy can be performed before the lens fragmentation. This change of sequence can reduce the surgical time to a considerable degree and thus increase the precision of the cataract procedure substantially.

In some detail, the cataract procedure **350** can include an imaging **360** of the capsule **222**, e.g. by an OCT imaging system, followed by a capsulotomy **370**, and completed by a lens fragmentation **380**. Since the capsulotomy **370** does not deform the lens **220**, there is no need for a second imaging, in contrast to the procedure **300**.

FIG. **9** illustrates an imaging-controlled cataract method **400** in more detail. The method **400** can include an imaging **410** of an imaged ophthalmic layer in an imaged region of an eye, followed by an identifying **420** of the coordinates of the imaged layer from the image. These tasks can be performed, for example, by the imaging system **122** of the imaging-based laser-controller **120**. The identifying **420** can include performing a feature-recognition analysis. In other cases, it can include receiving an operator-input through an operator interface **128**. These tasks can be performed by the imaging system **122**, the pattern generator **124** or the image analyzer **126**.

Next, the method **400** can include a generating **430** of coordinates of points of a scan-pattern, and a determining **440** of a distance of the points of the scan-pattern from the imaged layer. These steps can be performed for example, by the pattern generator **124**.

The method **400** can further include an associating **450** of laser-power parameters with the generated points based on their determined distance. The tasks **420** to **450** can include receiving possible inputs **422**-**452** from an operator of the laser system **100** through the operator interface **128**.

The method can also include a signaling **460** of the generated coordinates of the points of the scan-pattern to the beam scanner **116** and a signaling **470** of the corresponding laser-power parameters to the beam attenuator **114**.

FIG. **10** illustrates the case of surgical relevance when the lens capsule **222** has an uneven shape. This situation can arise in different circumstances. For example, the docking of the patient interface **136** can cause considerable deformation of the anterior segment of the eye **1**. Or an ophthalmic trauma or a prior lens fragmentation procedure can result in an uneven lens shape. In any of these circumstances, the laser system **100** can be capable of analyzing an image **256** of the imaged layer that exhibits more than two local extrema. Visibly, a simple sinusoidal model curve **258** is insufficient to identify the imaged layer and to determine its z-depth coordinate in this case. Therefore, embodiments of the imaging system **122**, the pattern generator **124** or the image analyzer **126** can be capable of recognizing the imaged layer and determine its z-depth coordinate even in this more challenging case, for example, by using sophisticated feature-recognition software. Having determined and characterized the image **256** of the imaged layer can allow the pattern generator **124** to define the tracking band **257** to associate laser-power parameters with the spots of the scan-pattern accordingly.

FIGS. **11**A-D illustrate that the imaging system **122** of the laser system **100** can image a region in the eye, the pattern generator **124** can generate coordinates of points of a scan-pattern for the beam scanner **116**, and associate a laser-power parameter with the points of the scan-pattern depending on a distance of the points from a target-pattern.

An example for such a target pattern can be a chop pattern **500**, including the chop-planes **500**-X and **500**-Y. Such chop patterns **500** can be used for lens fragmentation. FIG. **11**A illustrates the case when the z-axis of the lens **220** is aligned with the z-axis of the laser system **100**. In this case the chop-planes **500**-X and **500**-Y are also parallel to the z-axis of the laser system **100**.

FIG. **11**B illustrates that if the lens **220** is tilted relative to the z-axis of the laser system **100**, as illustrated e.g. in FIG. **4**B, then the chop planes **500**-Xt and **500**-Yt can be tilted as well. Since the scan-pattern often includes a first manifold of points at a first fixed z-depth, followed by a second manifold at a slightly lesser z-depth, the scan-pattern of tilted chop-planes with laser systems that cannot adjust the power of the laser pulses would create cuts into the capsular bag **222**, leading to massive surgical complications.

In contrast, embodiments of the laser system **100** can associate laser-parameters depending on the distance of the points of the scan-pattern from the chop planes **500**-Xt and **500**-Yt.

FIGS. **11**C-D illustrate the points of the scan-pattern with low and high laser power, generated by the pattern generator **124** to form the tilted **500**-Xt and **500**-Yt chop planes. Visibly, creating cuts by adjusting the power of the laser pulses depending on their proximity to the target-pattern can avoid cutting into the capsular bag—a major surgical advantage.

FIG. **11**D illustrates clearly that, as it was the case of the tracking band **257**, a photodisruptive laser-power parameter can be associated with scan-points that are closer to the target-pattern **500**-Xt and **500**-Yt than a predetermined distance Dcut, and a non-photodisruptive laser-power parameter with the scan-points that are farther from the target-pattern than the predetermined distance Dcut.

In other implementations, the cutting surface can be a circular surface-segment, a spiral surface-segment, a corneal access cut and a limbal relaxing cut.

FIGS. **12**A-B illustrate that in some cases the target pattern **260-2** can be a target volume with an axis tilted relative to an optical axis of the laser system **100**. Here, the scan pattern includes cylindrical patterns **260-1**, and the laser-power parameter of the points of this scan-pattern is adjusted to form a tilted volume cut **260-2**. Such a utility can be useful for correcting a refractive property of the lens **220**, for example.

In some implementations, the pattern generator **124** can be configured to associate the laser-power parameters with the points of the scan-pattern depending additionally on a distance of the points from an ophthalmic layer, imaged by the imaging system **122**.

While this specification contains many specifics, these should not be construed as limitations on the scope of the invention or of what can be claimed, but rather as descriptions of features specific to particular embodiments. Certain features that are described in this specification in the context of separate embodiments can also be implemented in combination in a single embodiment. Conversely, various features that are described in the context of a single embodiment can also be implemented in multiple embodiments separately or in any suitable subcombination. Moreover, although features can be described above as acting in certain combinations and even initially claimed as such, one or more features from a claimed combination can in some cases be excised from the combination, and the claimed combination can be directed to a subcombination or variation of a subcombination.

The invention claimed is:

1. An imaging-based laser system, comprising:

a laser-beam system, including

a laser engine, configured to generate a beam of laser pulses,

a beam attenuator, configured to modify a laser-power parameter of the laser pulses, wherein the laser-power parameter is one of a pulse energy, a pulse power, a pulse length and a pulse repetition rate, and

a beam scanner, configured to scan the beam to points of a cylindrical scan-pattern in an eye; and

an imaging-based laser-controller, configured to:

image a layer in the eye that is tilted relative to an optical axis of the laser system,

determine z-depths of a sequence of points in the cylindrical scan-pattern that correspond to the imaged layer in the eye,

generate a tracking band within the cylindrical scan pattern defining a cut to be made in the eye, wherein a lower boundary of the tracking band has a non-uniform z-depth that varies according to the determined z-depths of the sequence of points corresponding to the imaged layer,

cause the beam scanner to scan the beam of laser pulses to the points of the cylindrical scan-pattern, and

cause the beam attenuator to control the laser-power parameter of the laser pulses such that a laser power parameter of laser pulses in the tracking band is above a photo-disruption threshold, and a laser power parameter of laser pulses outside the tracking band is below the photo-disruption threshold.

2. The laser system of claim **1**, the beam attenuator comprising at least one of:

a Pockels cell, a polarizer-assembly, a mechanical shutter, an electro-mechanical shutter, and an energy wheel.

3. The laser system of claim **1**, wherein:

the beam attenuator is disposed between the laser engine and the beam scanner in a path of the beam.

4. The laser system of claim **1**, wherein:

the beam attenuator is disposed after the beam scanner in a path of the beam.

5. The laser system of claim **1**, wherein:

the beam attenuator is part of the laser engine.

6. The laser system of claim **1**, wherein:

the beam attenuator and the beam scanner are at least partially integrated.

7. The laser system of claim **1**, the laser-controller comprising:

an imaging system, configured to image the imaged layer in the eye; and

a pattern generator, configured to:

generate coordinates of each point within the cylindrical scan-pattern,

associate a particular laser-power parameter with each point in the cylindrical scan pattern based on the tracking band, and

signal the generated coordinates of each point to the beam scanner, and

signal the particular laser-power parameter of each point to the beam attenuator.

8. The laser system of claim **7**, the imaging system comprising:

at least one of an ophthalmic coherence tomography system, a Scheimpflug imaging system, a scanning imaging system, a single shot imaging system, an ultrasound imaging system, and a video imaging system.

9. The laser system of claim **7**, wherein:

the imaging system is configured to image the imaged layer in an image region, wherein the image region

is based on one of a loop, an arc, a line, and a two-dimensional pattern transverse to an axis of the imaging system, and

extends to an image depth along the axis of the imaging system.

10. The laser system of claim **7**, wherein:

the imaging system is configured to support a determination of a z-depth coordinate of the imaged layer corresponding to a scanning coordinate along an image-scan.

11. The laser system of claim **10**, wherein:

the laser system comprises an operator interface; and

the imaging system is configured to support the determination of the z depth coordinate of the imaged layer using an input from an operator through the operator interface.

12. The laser system of claim **11**, wherein:

the operator interface is configured to assist the operator to fit a model curve to the image of the imaged layer.

13. The laser system of claim **11**, wherein:

the operator interface is capable of receiving the operator-input from at least one of a keyboard, a touch-screen, a computer-communication channel, an external memory, a flash-drive, an internet connection, a speech-recognition apparatus and a wireless connection.

14. The laser system of claim **10**, wherein:

the imaging system is configured to determine the z-depth coordinate of the imaged layer by performing a feature-recognition analysis of the image of the imaged layer.

15. The laser system of claim **14**, wherein:

the imaging system is configured to utilize at least one of a result of a pre-surgery measurement, statistical data, video image data, ophthalmic coherence tomography image data,

and a model-based computation during the determination of the z-depth.

16. The laser system of claim **10**, wherein:

the imaging system is configured to forward the z-depth and scanning coordinates of the imaged layer to the pattern generator; and

the pattern generator is configured

to determine the distance of the points of the scan-pattern from the imaged layer based on the forwarded coordinates of the imaged layer and the generated coordinates of the points,

to associate a first laser-power parameter above a photodisruption threshold with a first set of points closer to the imaged layer than a predetermined distance, and

to associate a second laser-power parameter below a photodisruption threshold with a second set of points farther from the imaged layer than the predetermined distance.

17. The laser system of claim **10**, wherein:

the imaging system is configured to forward the z-depth and scanning coordinates of the imaged layer to the pattern generator; and

the pattern generator is configured

to determine the distance of the points of the scan-pattern from the imaged layer based on the forwarded coordinates of the imaged layer and the generated coordinates of the points, and

to associate with the coordinates of the points a laser-power parameter that is a decreasing function of the distance of the points from the imaged layer.

18. The laser system of claim **7**, wherein:

the imaging system is configured to forward the image of the imaged layer to the pattern generator; and

the pattern generator is configured

to receive the image from the imaging system, and

to determine a z-depth coordinate of the imaged layer corresponding to a scanning coordinate along an image scan.

19. The laser system of claim **18**, wherein:

the pattern generator is configured to determine the z-depth of the imaged layer in part by performing a feature-recognition analysis of the received image of the imaged layer.

20. The laser system of claim **18**, wherein:

the pattern generator is configured to receive an operator input through an operator interface during the process of determining the z-depth of the imaged layer.

21. The laser system of claim **20**, wherein:

the operator interface is capable of receiving the operator-input from at least one of a keyboard, a touch-screen, a computer-communication channel, an external memory, a flash-drive, an internet connection, a speech-recognition apparatus and a wireless connection.

22. The laser system of claim **18**, wherein:

the pattern generator is configured to:

generate the tracking band as a manifold of points within a predefined distance from the coordinates of the imaged layer;

associate a laser-power parameter above a photodisruption threshold with points of the scan-pattern inside the tracking band, and

to associate a laser-power parameter below a photodisruption threshold with points of the scan-pattern outside the tracking band.

23. The laser system of claim **7**, the laser controller comprising:

an image analyzer, configured to determine a z-depth coordinate of the imaged layer corresponding to a scanning coordinate along an image-scan.

24. The laser system of claim **23**, wherein:

the image analyzer is configured to determine the z-depth coordinate of the imaged layer by performing a feature-recognition analysis of the image of the imaged layer.

25. The laser system of claim **23**, wherein:

the image analyzer is configured to determine the z-depth coordinate of the imaged layer by receiving an operator input through an operator-interface.

26. The laser system of claim **23**, wherein:

the image analyzer is at least partially integrated with one of the imaging system and the pattern generator.

27. The laser system of claim **1**, wherein:

the imaged layer is a lens capsule between a lens of an eye and an aqueous anterior chamber of the eye;

the scan-pattern corresponds to a cylindrical capsulotomy cut intersecting the lens capsule; and

the imaging-based laser controller is configured to:

associate a photodisruptive laser-power parameter with points inside a tracking band related to the intersection of the cylindrical capsulotomy cut and the lens capsule, and

associate a non-photodisruptive laser-power parameter with points outside the tracking band.

28. The laser system of claim **27**, wherein:

the laser system is configured to perform a capsulotomy before a lens fragmentation during a cataract procedure.

29. The laser system of claim **27**, wherein:

the imaging-based laser controller is configured to to analyze an image of the capsule boundary layer with more than two local extrema by at least one of a pattern generator and an image analyzer.

* * * * *